

Review

# Catalytic Conversion of Levulinic Acid into 2-Methyltetrahydrofuran: A Review

Sreedhar Gundekari <sup>1,\*</sup>  and Sanjib Kumar Karmee <sup>2,\*</sup> 

<sup>1</sup> Department of Engineering Chemistry, Koneru Lakshmaiah Education Foundation, KL (Deemed to be) University, R.V.S Nagar, Moinabad-Chilkur Rd, Aziznagar 500075, Telangana, India

<sup>2</sup> The Odisha Renewable Energy Research Institute (ORERI), Subarnapur 767018, Odisha, India

\* Correspondence: sreedhar.gundekari@gmail.com or sreedhar.gundekari@klh.edu.in (S.G.); sanjibkarmee@gmail.com (S.K.K.)

**Abstract:** Biomass-derived furanics play a pivotal role in chemical industries, with 2-methyltetrahydrofuran (2-MTHF), a hydrogenated product of levulinic acid (LA), being particularly significant. 2-MTHF finds valuable applications in the fuel, polymer, and chemical sectors, serving as a key component in P-series biofuel and acknowledged as a renewable solvent for various chemical processes. Numerous research groups have explored catalytic systems to efficiently and selectively convert LA to 2-MTHF, using diverse metal-supported catalysts in different solvents under batch or continuous process conditions. This comprehensive review delves into the impact of metal-supported catalysts, encompassing co-metals and co-catalysts, on the synthesis of 2-MTHF from LA. The article also elucidates the influence of different reaction parameters, such as temperature, type and quantity of hydrogen source, and time. Furthermore, the review provides insights into reaction mechanisms for all documented catalytic systems.

**Keywords:** biomass; furanic molecules; levulinic acid; 2-methyltetrahydrofuran; hydrogenation



**Citation:** Gundekari, S.; Karmee, S.K. Catalytic Conversion of Levulinic Acid into 2-Methyltetrahydrofuran: A Review. *Molecules* **2024**, *29*, 242. <https://doi.org/10.3390/molecules29010242>

Academic Editors: Juan Antonio Cecilia and Nan Zhao

Received: 22 October 2023  
Revised: 14 December 2023  
Accepted: 28 December 2023  
Published: 2 January 2024



**Copyright:** © 2024 by the authors. Licensee MDPI, Basel, Switzerland. This article is an open access article distributed under the terms and conditions of the Creative Commons Attribution (CC BY) license (<https://creativecommons.org/licenses/by/4.0/>).

## 1. Introduction

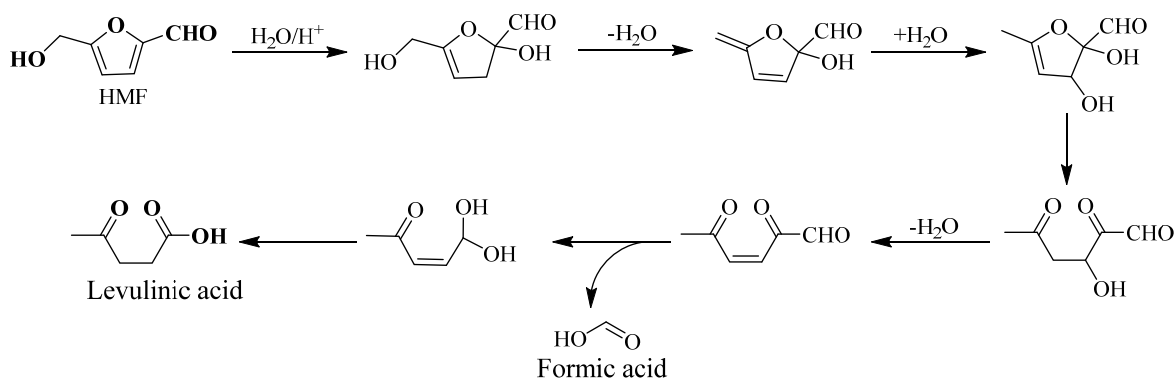
Furanic molecules, also known as furans, are a significant group of organic compounds distinguished by a cyclic structure consisting of a five-membered ring composed of four carbon atoms and one oxygen atom. These compounds are known to have diverse applications in the chemical industries, and their significance is heightened by their potential as renewable chemicals obtained from biomass [1,2]. Biomass materials, viz. wood, agricultural remnants, and plant substances, act as a sustainable reservoir for generating furanic molecules. The conversion of biomass into furans involves a spectrum of chemical processes, including dehydration and decarboxylation reactions [3,4]. The utilization of biomass as a precursor is advantageous due to its renewable nature, and in the context of diminishing reliance on fossil-derived fuels and chemicals [5,6]. Furanic molecules from biomass play a crucial role in the realms of green chemistry and the sustainable development of society. They serve as basic components for producing a variety of valuable substances and materials, spanning pharmaceuticals, polymers, resins, and solvents [7]. Moreover, furanic compounds possess the potential to supplant conventional petrochemical-based products, thereby fostering a more ecologically balanced and sustainable future [8]. In the pursuit of environmentally benign practices, researchers and scientists are continuously exploring novel techniques to effectively extract furanic molecules from bio-resources [9]. These endeavors aim to optimize conversion methods and discover new applications for these bio-based compounds. By unlocking the potential of furanic molecules from biomass, one can actively contribute to shaping the chemical industries that are not only sustainable but also environmentally vigilant [10]. Among the biomass-based furanic compounds, 2-hydroxymethylfurfural (HMF) and furfural play an important role in building a biorefinery. HMF and furfural are furanic compounds synthesized from biomass

that have garnered significant attention among the scientific and industrial communities due to their diverse applications and potential as renewables [11,12].

HMF, a valuable furanic compound, is derived from sugars obtained from biomass, such as glucose, and fructose. Its production typically involves acid-catalyzed dehydration of the mentioned sugars [13,14]. Furfural, another valuable furanic compound derived from biomass, is primarily sourced from agricultural residues, such as corn cobs, oat hulls, and sawdust. Its production often involves the acid-catalyzed dehydration of pentose sugars, such as xylose [15]. Several factors, including the type and concentration of the acid catalyst, reaction temperature, and reaction time, can influence the efficiency of the reaction and the yield of HMF and furfural from sugars. It is crucial to optimize these reaction parameters to maximize the yield of HMF and furfural while minimizing the formation of other products [16,17]. Moreover, ongoing research explores novel catalytic processes and alternative feedstocks with the aim of improving the efficiency and sustainability of HMF and furfural production methods.

HMF and furfural serve as precursors for the synthesis of Levulinic acid (LA) [18]. LA plays a crucial role as a primary precursor in catalytic transformations for the production of fuels and chemicals [19,20]. LA, characterized by the molecular formula  $C_5H_8O_3$ , can be obtained as a white crystalline solid below 30 °C. It exhibits solubility in both water-based solutions and typical organic solvents, including polar variants [19].

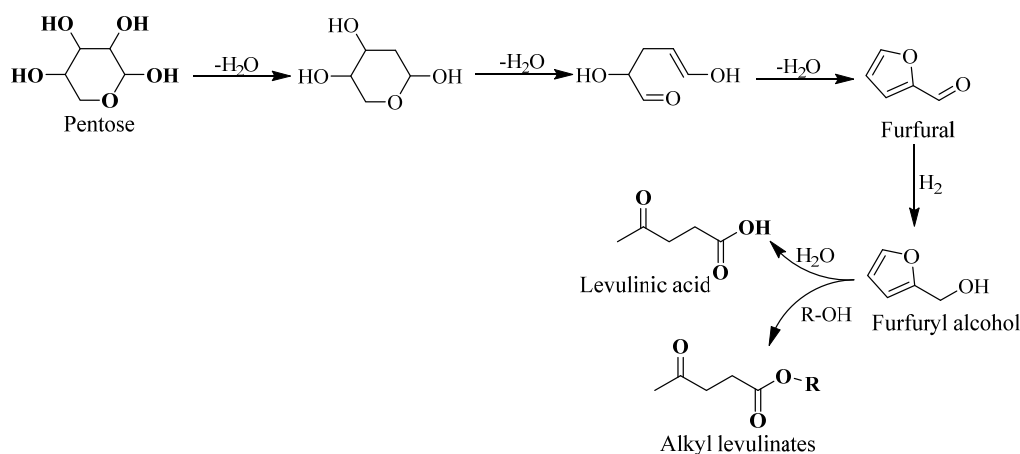
LA is produced from glucose derived from cellulose in a two-step process. Initially, glucose undergoes isomerization to fructose, which is then dehydrated to generate HMF. In the subsequent step, HMF undergoes hydrolysis in an aqueous environment, resulting in the formation of LA with formic acid produced as a byproduct (Scheme 1) [21]. In the presence of an alcoholic medium, conversion leads to the formation of alkyl levulinates and alkyl formates [19]. LA can also be synthesized from furfural through an intermediate step involving furfuryl alcohol. Furfural is selectively hydrogenated to furfuryl alcohol using metal-supported catalysts. In the presence of water, furfuryl alcohol is transformed into LA and levulinic esters (alkyl levulinates) while using an alcoholic medium (Scheme 2) [22]. In general, the conversion of hydroxymethyl furfural (HMF) and furfuryl alcohol into LA is catalyzed by different acid catalysts, viz. solid acids, acidic ionic liquids, and mineral acids [23].



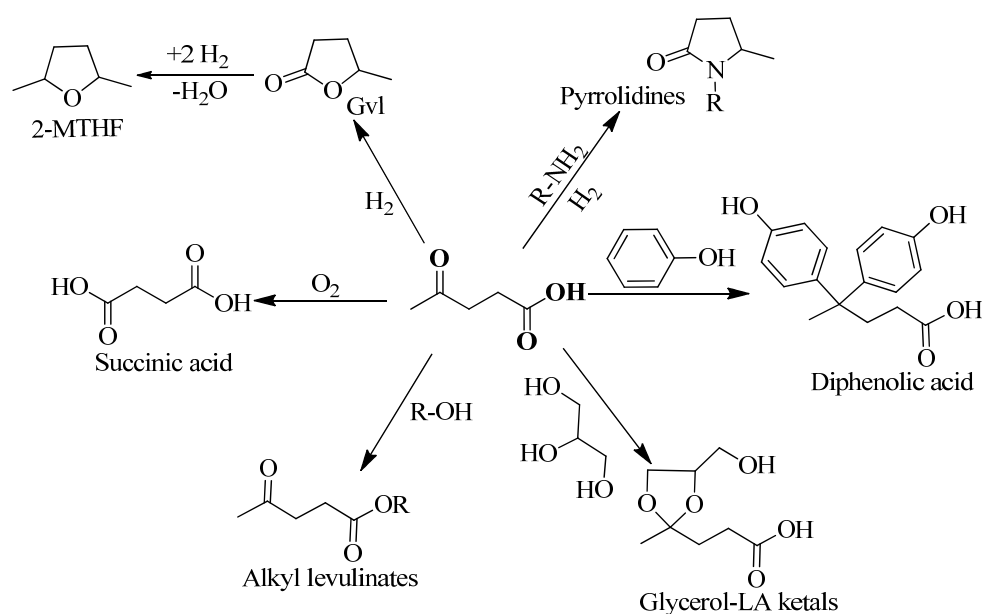
**Scheme 1.** Mechanism of the reaction for synthesizing LA from HMF. Scheme taken from Gundekari et al. [20].

LA possesses diverse functional groups, including carboxyl, carbonyl, and methylene, rendering it highly versatile and suitable for a wide range of organic reactions. These reactions include hydrocyclization, hydrogenation, dehydration, oxidation, reductive amination, halogenation, alkylation, and condensation, as illustrated in Scheme 3. LA can act as an intermediate in the synthesis of many compounds, including arylated cyclic lactones, alkylated lactones, ketals, halo substituted keto carboxylic acids, amides (cyclic/acyclic), valerates, valeric acids, aliphatic alcohols, acid halides, 1,4-diketones, alkanes, alkenes, cyclic ethers, and numerous other derivatives [24–27]. LA contains oxygen functionality

(oxo and carboxylic), leading to the production of numerous high-value products through hydrocyclization and hydrodeoxygenation reactions [28]. When exposed to the H<sub>2</sub> environment, LA primarily yields valuable products like 2-methyltetrahydrofuran (2-MTHF), 1,4-pentanediol (1,4-PDO), and  $\gamma$ -valerolactone (Gvl). The particular product is contingent on the catalytic system and the parameters of the reaction [29–32].



**Scheme 2.** Mechanism of the reaction for synthesizing LA from furfural through the intermediate furfuryl alcohol. Scheme taken from Gundekari et al. [20].



**Scheme 3.** Catalytic organic transformations of LA. Scheme taken from Gundekari et al. [20].

The hydrogenated derivatives of LA play a crucial role in industry. For example, Gvl is a valuable platform chemical used in diverse applications, such as the preparation of biofuels like valerates, non-functionalized aromatic hydrocarbons, butanes, and liquid alkanes (Scheme 4) [33–36]. It also acts as an intermediate for polymers like 1,4-PDO, adipic acid, and  $\alpha$ -methylene- $\gamma$ -valerolactone [37–39]. Additionally, Gvl serves as an eco-friendly solvent in organic reactions, including the conversion of lignocellulose components [40,41]. Through sequential hydrogenation, LA transforms into 1,4-PDO via Gvl as an intermediate. Under high temperatures and acidic conditions, 1,4-PDO cyclizes to form 2-MTHF. 1,4-PDO also serves as a monomer in the production of essential polymers like polyesters, polyurethanes, and polyethers, which are utilized in textiles, adhesives, coatings, and flexible foams. Additionally, 1,4-PDO acts as a solvent in applications involving coatings,

dyes, and printing inks [42]. Another hydrogenated product of LA, 2-MTHF, is gaining prominence in various industries due to its significant chemical properties [43–45].

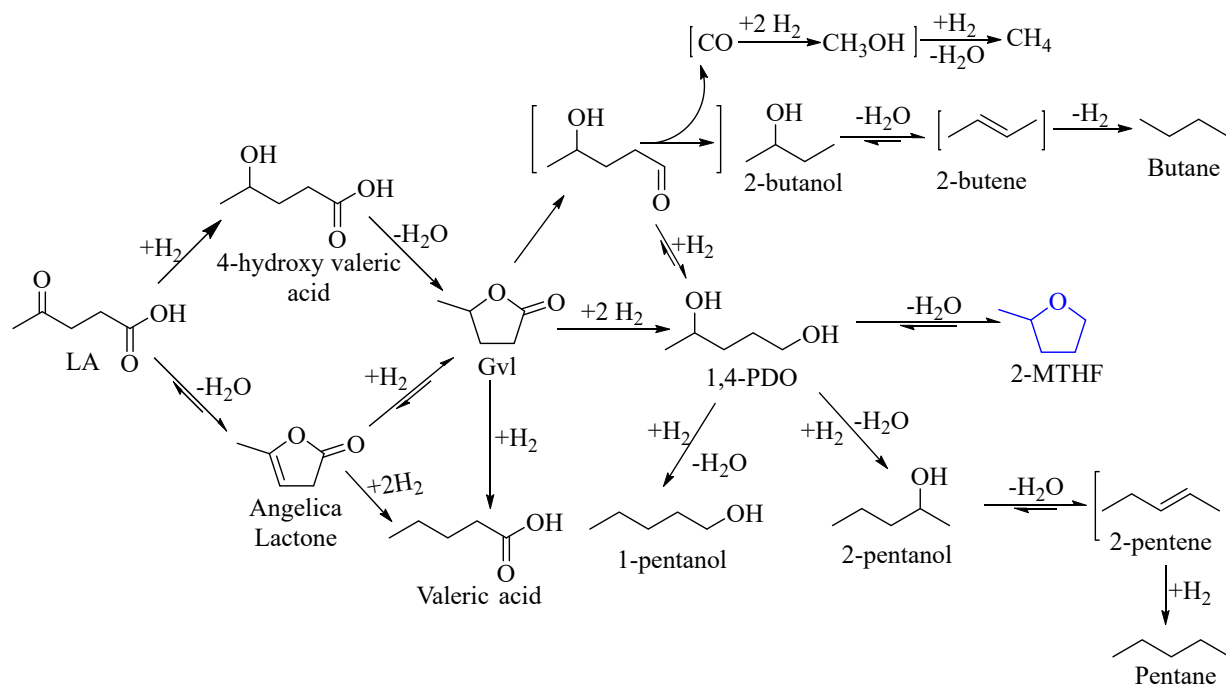
This contribution focuses on catalytic methods for the conversion of LA under a hydrogen ( $H_2$ ) atmosphere, with an emphasis on the selective synthesis of 2-MTHF. The study thoroughly investigates and compiles the influence of diverse metal catalysts, catalytic supports, and reaction parameters pertaining to this conversion process, and documentation of the findings. The review concludes by highlighting insights of the subject by critically analyzing the reported catalytic systems, and challenges in this research area are also elaborated.

## 2. 2-Methyltetrahydrofuran (2-MTHF)

2-MTHF is a saturated cyclic ether, also known as a heterocyclic compound due to its oxygen atom within the ring structure. Chemically, it is represented as  $C_5H_{10}O$ , and its molecular formula indicates its close relation to tetrahydrofuran (THF), a commonly used solvent. As of 2021, the global market value of 2-MeTHF is anticipated to reach USD 3.4 billion, with a projected increase of USD 4.4 billion by 2030. Although its industrial production is currently on a modest scale, there is a growing demand for large-scale manufacturing. Envisaging an annual production of 9.1 million kg, a sizable production facility could potentially generate around USD 102 million in annual revenue. The US Department of Energy has classified 2-MTHF as a 'P-Series fuel' due to its impressive fuel characteristics. Its hydrophobic properties, high heating value, and elevated specific gravity allow it to be blended with gasoline up to 70% [46,47].

### 2.1. Preparation of 2-MTHF from LA

Typically, the manufacturing of 2-MTHF involves two separate methods: sequential hydrogenation of furfural and LA. In the first process, the furfural undergoes hydrogenation to produce 2-methylfuran (2-MF), which is subsequently further hydrogenated to result in 2-MTHF [48]. This reaction involves the introduction of hydrogen gas ( $H_2$ ) in the presence of suitable metals (such as Nickel, Palladium, Copper, Ruthenium) supported on appropriate materials like alumina ( $Al_2O_3$ ), silica ( $SiO_2$ ), and activated carbon [49]. The production of 2-MTHF from LA comprises essential stages, such as hydrogenation, dehydration, and hydrocleavage processes, with key intermediates like Gvl and 1,4-PDO. Throughout this reaction, various side products might form, including valeric acid, pentanols, butanol, pentane, and butane (Scheme 4) [50]. In the initial stage, LA undergoes hydrocyclization, a process in which it cyclizes with the aid of a suitable catalyst. This stage leads to the generation of an intermediate compound, often Gvl. This intermediate, such as Gvl, then undergoes a hydrogenolysis reaction in which hydrogen gas ( $H_2$ ) is used to break the chemical bond (C-O). This process results in the formation of 1,4-PDO, which can undergo subsequent cyclization under acidic reaction conditions, ultimately yielding 2-MTHF as the desired end product (Scheme 4). The preparation of 2-MTHF from the two raw materials, LA and furfural, reveals that the conversion of LA to 2-MTHF is more efficient than furfural to 2-MTHF for several reasons. First, raw materials for LA, such as cellulose, are abundant compared to the xylose source used in furfural preparation. This abundance contributes to the effectiveness of the LA to 2-MTHF process. Additionally, the selectivity of 2-MTHF from LA is more pronounced compared to that from furfural. The hydrogenation of furfural to 2-MTHF generates various side products, including Cyclopentanone, furfuryl alcohol, tetrahydrofurfuryl alcohol, 2-methylfuran, tetrahydrofurfural, 1,2-pentanediol, and 1,5-pentanediol. On the other hand, the conversion of LA to 2-MTHF results in only Gvl and 1,4-pentanediol as side products, demonstrating a higher selectivity for 2-MTHF in this process. Furthermore, the conversion of furfural to 2-MTHF requires a substantial amount of  $H_2$  (4 equivalents), whereas the LA to 2-MTHF conversion necessitates only 3 equivalents of  $H_2$ . This reduced hydrogen consumption adds to the overall efficiency of the LA to the 2-MTHF pathway.



**Scheme 4.** Reaction network of LA under  $H_2$  environment. Scheme adopted from [50].

The conversion of LA into 2-MTHF stands as a vibrant area of research within the fields of green chemistry and biofuels [51]. In recent research efforts, scientists have focused on investigating various catalysts, reaction conditions, and methods aimed at the efficient conversion of LA into 2-MTHF. Researchers have extensively investigated the use of metal catalysts, acid catalysts, and their combinations to facilitate this conversion. Furthermore, these investigations have involved a wide range of feedstocks, along with variations in reaction temperatures, pressures, and solvent systems, all aimed at optimizing the yield and selectivity of 2-MTHF. Section 3 provides a critical review of the conversion of LA to 2-MTHF using various catalysts.

In the hydroconversion of LA to 2-MTHF, batch experiments were carried out using a high-pressure reactor constructed from either Hastelloy C-276 or stainless steel (SS-316). The reactor underwent thorough examination to optimize the reaction parameters, including temperature, pressure, and reaction time. Initially, the reactor vessel was loaded with the catalyst. Following this, the substrate (LA) dissolved in either water or an organic solvent was introduced into the vessel. The system underwent three purges with nitrogen ( $N_2$ ) or hydrogen ( $H_2$ ) before pressurization/feeding with a fixed amount of  $H_2$ . The reaction was then conducted at the desired temperature and duration. After completion, the reactor was cooled to room temperature, and excess  $H_2$  was released. The catalyst was separated through simple centrifugation. Quantitative analysis of the product mixture was typically carried out using Gas Chromatography (GC) and/or Gas Chromatography-Mass Spectrometry (GC-MS) [52].

In continuous hydrocyclization experiments converting LA to 2-MTHF, a stainless steel fixed-bed catalytic reactor was typically employed [53]. The continuous reactor setup included a pre-heater for vaporizing or heating the liquid feed, and an assembly comprising a reactor and a furnace in the upstream section. The downstream section comprised a condenser and a gas-liquid separator. The reactor tube featured temperature thermocouples with transmitters. The catalytic reactor bed was enclosed within a furnace and heated electrically. Initially, the reactor was loaded with the catalyst. The loaded catalyst was pre-heated at a specific temperature and duration until the physisorbed  $H_2O$  molecules were removed from the catalyst. Various parameters such as column temperature, pre-heater temperature, liquid flow rate (for LA in solvent), hydrogen ( $H_2$ ) feed flow (monitored and controlled using a Mass Flow Controller), and  $H_2$  pressure in the reactor were systematically

adjusted for optimizing the reaction. Under the optimized conditions, the reaction was carried out for a specific time to assess the stability and activity of the catalyst. Throughout the reaction, the product mixture was condensed and separated. The collected product was then analyzed using GC or GC-MS.

## 2.2. Properties of 2-MTHF

2-Methyltetrahydrofuran (2-MeTHF) is a chemical compound that possesses several important properties [54–56]. The key and important 2-MTHF properties are mentioned below. These properties make 2-MTHF suitable for a range of applications, including as a solvent in various chemical reactions [57], as a component in fuel formulations [58,59], and in other industrial processes.

2-MTHF is classified as a polar aprotic solvent, signifying its partial polarity due to the presence of an oxygen atom in its structure while lacking acidic hydrogen atoms. This characteristic renders it suitable for a broad spectrum of chemical reactions. Under typical conditions, 2-MTHF exhibits stability; however, its reactivity depends on the presence of specific reagents or catalysts in particular reaction setups [55]. Although generally considered to have low toxicity, prudent handling is essential, as with any chemical substance. It is notably less toxic than common solvents like tetrahydrofuran (THF) and dichloromethane (DCM). Regarded as environmentally friendly, 2-MTHF boasts a lower environmental impact than some counterparts and finds applications in green chemistry initiatives. Despite these advantages, it is crucial to handle 2-MTHF with care due to its flammability; it possesses a relatively low flash point, making it susceptible to ignition at moderate temperatures [60,61].

## 2.3. Applications of 2-MTHF

2-MeTHF plays a crucial role in the fuel industry, serving as a component in alternative fuels and a solvent for fuel-related processes. Specifically, it is utilized in P-series biofuels, a family of alternative fuels designed by the U.S. Department of Energy, to reduce greenhouse gases and promote renewable energy in transportation [62]. Additionally, 2-MeTHF functions as a solvent in the production of biofuels and can be used as a fuel additive to enhance combustion efficiency and reduce emissions [63,64]. It is also employed in fuel blending to improve properties like octane rating [64,65], and in fuel cell research, particularly in Li-ion batteries [66–68]. 2-MTHF serves as a green solvent in organic reactions, acting as an eco-friendly alternative to conventional solvents like tetrahydrofuran (THF) in various processes such as Grignard reactions and Suzuki-Miyaura cross-coupling reactions [55,57,69–71]. In the pharmaceutical industry, it finds application in peptide synthesis, aiding in solid-phase peptide synthesis and the preparation of peptide-based drugs [60,72]. Additionally, 2-MTHF is utilized for crystallization and purification of pharmaceutical compounds [63], dissolution testing in quality control [73,74], and as a solvent in the formulation of Active Pharmaceutical Ingredients (APIs) to enhance bioavailability [73,75,76]. In the agro-chemical industry, 2-MTHF is utilized as a solvent in the formulation of pesticides, herbicides, and insecticides, facilitating the dissolution and stabilization of active ingredients for effective and stable formulations [77]. Additionally, it finds application in the extraction and isolation of bioactive compounds from plant components, supporting the development of pesticides that use natural products as starting materials [54,78]. Moreover, in the field of electrochemistry, 2-MTHF serves as an electrolyte solvent, enhancing the performance and stability of electrochemical cells like lithium-ion batteries and fuel cells, particularly in improving low-temperature battery performance [67,68,79]. Additionally, it finds application as a solvent in various electrochemical techniques for redox reactions [80,81], electrodeposition, and electroplating processes [82]. 2-MTHF is also used in redox flow batteries, contributing to more efficient and cost-effective energy storage solutions [83], and as a reaction medium for electrochemical synthesis of organic compounds due to its favorable properties [84]. In the polymer industry, 2-MTHF serves as a versatile solvent for polymerization, contributing to the production of elastomers and thermoplastic

polyurethanes [85]. It also functions as a polymerization initiator, controlling the properties of the formed polymers and enhancing the processability of certain thermoplastic polymers during extrusion and molding [86–88]. Additionally, 2-MTHF is employed as a solvent in polymer characterization methods [89,90] and plays a role in polymer recycling processes by aiding in the dissolution and separation of specific polymers from mixed plastic waste for material recovery [91,92]. In extraction and separation processes, 2-MTHF is utilized for its solvating properties, finding application in the extraction of natural products and the purification of organic compounds. It serves as a chromatographic solvent in both high-performance liquid chromatography (HPLC) and gas chromatography (GC), facilitating the separation of diverse compounds [93]. Additionally, 2-MTHF acts as an extraction solvent for isolating natural products, pharmaceutical compounds, and other target molecules from complex matrices [94], and is employed in liquid-liquid extraction processes to separate components based on their differential solubility in the organic phase [78,95].

### 3. Catalytic Conversion of LA to 2-MTHF

In this segment, an in-depth analysis is presented on the catalytic systems reported for the hydro-conversion of LA to 2-MTHF. The discussion encompasses diverse catalytic systems, explores the impact of parameters and co-catalysts, and delves into the intricacies of the reaction mechanism.

Upare et al. reported vapor phase hydrocyclization of LA to 2-MTHF using Nanocomposite Copper/Silica Catalyst in the presence of 1,4-dioxane at 265 °C and moderate H<sub>2</sub> pressure [53]. In this study, the impact of H<sub>2</sub> pressure and the weight percentage of the metal catalyst on 2-MTHF selectivity was investigated. At 265 °C and 1 bar H<sub>2</sub> pressure, the 5 wt% Cu/SiO<sub>2</sub> catalyst achieved full LA conversion, with 94% selectivity towards Gvl. Elevating the H<sub>2</sub> pressure to 10 bar resulted in a substantial increase in Gvl selectivity, reaching 99.9%. However, with further pressure increments, the selectivity shifted towards 1,4-PDO by reducing the Gvl selectivity to 93%. To attain the selectivity of 2-MTHF, the authors studied wt% of Cu on SiO<sub>2</sub> and found that increasing the wt% of Cu (from 5 wt% to 80 wt%) increased the selectivity of 2-MTHF and observed 64% of 2-MTHF at 80 wt% Cu/SiO<sub>2</sub> (Table 1, entry 1 to 4). The highest selectivity of 2-MTHF (89%) resulted from the addition of Ni-metal to the Cu/SiO<sub>2</sub> (8 wt% Ni–72 wt% Cu/SiO<sub>2</sub>), here the Ni metal act as a promoter and which enhanced the selectivity of 2-MTHF (Table 1, entry 5). Surprisingly, the Ni-Cu(72)/SiO<sub>2</sub> exhibited exceptional selectivity towards 2-MTHF, reaching 89% without any notable decline in catalytic activity over a period of 320 h. This result highlights the advantageous impact of nickel on enhancing selectivity. Moreover, the leaching of Cu metal is not observed in this reaction and exhibits minimal sintering of metals during the reaction, which was observed in various physicochemical techniques.

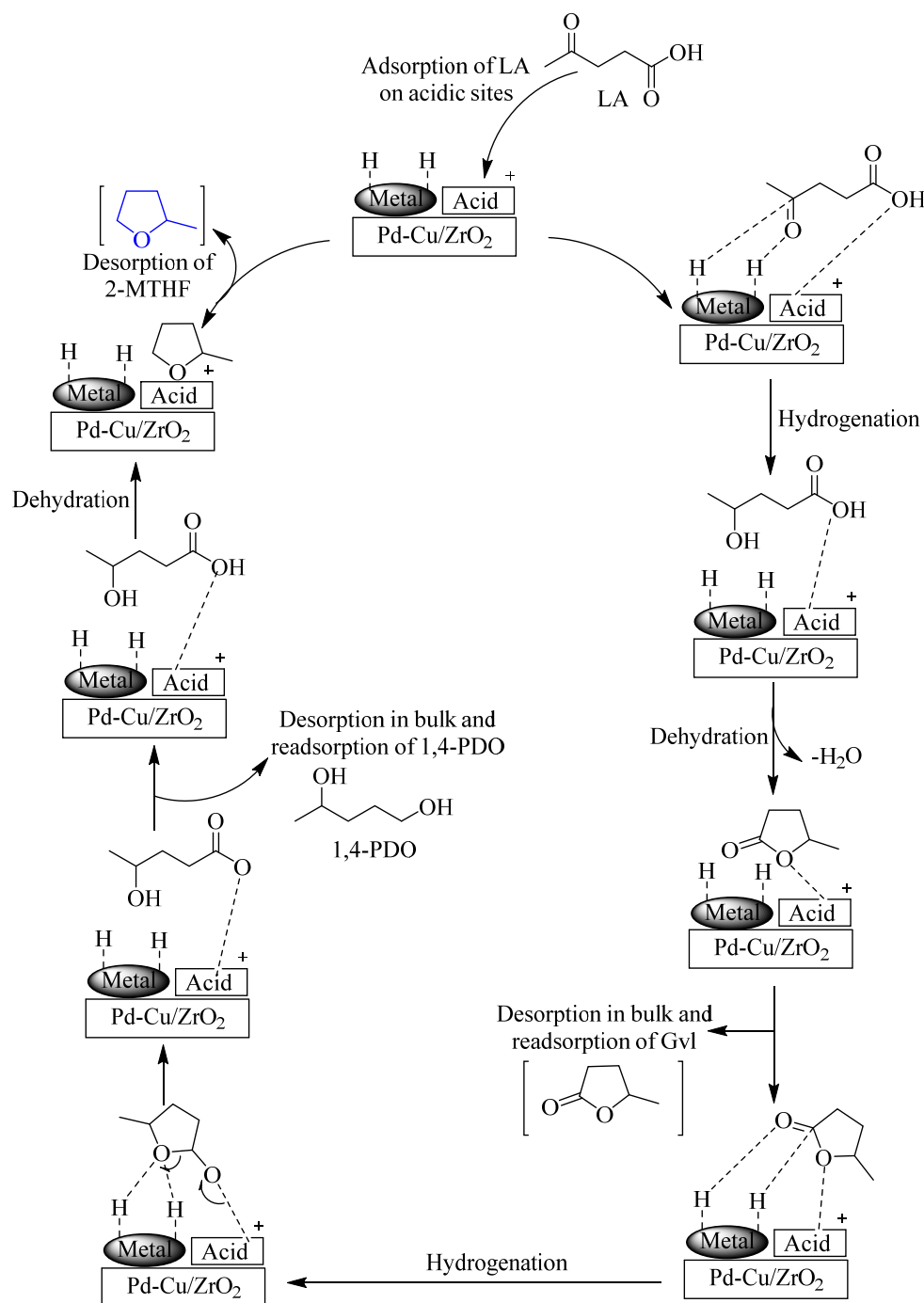
The Luque research group successfully developed a method for producing 2-MTHF from LA using both microwave and continuous flow processes, eliminating the need for molecular hydrogen. In this innovative approach, formic acid was employed as a hydrogen source [96]. Notably, formic acid was utilized as a co-product generated during the preparation of LA from glucose. Formic acid is an alternative source to produce in-situ H<sub>2</sub> by its decomposition during the reaction. Under microwave irradiation (150 °C temperature, 30 min microwave irradiation, 300 W), the authors screened several catalysts for this conversion, such as Ru-Starbon<sup>®</sup>, Rh-Starbon<sup>®</sup>, Pd-Starbon<sup>®</sup>, Cu-MINT, and Pd/C, among the catalysts used, the Cu-MINT catalyst showed high conversion, and Pd-based catalysts showed high selectivity towards 2-MTHF (Table 1, entry 6–10). Under continuous flow conditions, the Cu-MINT and Pd/C exhibited similar activities (79% and 73% conversion of LA) and showed significantly different selectivities toward 2-MTHF. In the Cu-MINT system, only two primary products were observed: 2-MTHF and 1,4-PDO, with selectivities of 60% and 40%, respectively. In contrast, the Pd/C system, though equally active, yielded a range of hydrogenation products, including 1,4-PDO, pentanoic acid (PA), and 4-hydroxyvaleric acid (HVA), with a limited selectivity towards 2-MTHF (<30 mol%). Further, they studied the stability of the Cu-MINT catalyst under a continuous process, and

the catalyst experienced significant deactivation over time on stream, rendering it unstable in these flow conditions. Further studies on catalyst leaching revealed the presence of substantial amounts of leached copper in the solution (identified by ICP). Notably, these leached copper species exhibited a light blue color typical of  $\text{Cu}^{2+}$  ions, providing clear evidence of catalyst deactivation through leaching.

The Miller research group introduced homogenous catalysts (Ru-based complexes) for catalyzing the stepwise hydrogenation of levulinic acid (LA) to produce 2-methyltetrahydrofuran (2-MTHF) through intermediates Gvl and 1,4-PDO [97]. Two distinct catalytic systems employing branched triphosphine ligands, namely, Triphos ( $\text{CH}_3\text{C}(\text{CH}_2\text{PPh}_2)_3$ ) and Ntriphos ( $\text{N}(\text{CH}_2\text{PPh}_2)_3$ ), were investigated. Among these, the most effective catalyst was found to be the pre-formed ruthenium species  $[\text{RuH}_2(\text{PPh}_3)\text{-}\{\text{N}(\text{CH}_2\text{PPh}_2)_3\text{-}\kappa_3\text{P}\}]$ . This catalyst accomplished almost total conversion of LA to 1,4-PDO without requiring any acidic additives, and it generated 87% 2-MTHF when employed in combination with  $\text{HN}(\text{Tf})_2$  (Table 1, entry 11). Various acidic additives were examined to enhance the conversion of 1,4-PDO to 2-MTHF. Among them,  $\text{HN}(\text{Tf})_2$  was the sole effective additive, while  $\text{NH}_4\text{PF}_6$  and paratoluenesulfonic acid (p-TsOH) had adverse effects.

Obregún et al. described the effectiveness of Ni- and Cu-based catalysts in converting LA to 2-MTHF in the presence of eco-friendly solvents such as  $\text{H}_2\text{O}$ , ethanol, 1-butanol, and 2-propanol at 250 °C and 70 bar  $\text{H}_2$  pressure over 5 h (Table 1, entries 12 to 15) [52]. Among these solvents, 2-propanol stood out as the most efficient, owing to its favorable thermodynamic dehydrogenation pathway, which is crucial for providing adequate hydrogen for the reaction. Unlike the other alcohols and  $\text{H}_2\text{O}$  medium, 2-propanol yielded the highest corresponding 2-MTHF. It has already been proven that Ni-based catalysts are known for their proficiency in dehydrogenating secondary alcohols into ketones and hydrogen, benefited significantly from 2-propanol's unique properties. From the experimental results, the authors revealed that, the Ni/ $\text{Al}_2\text{O}_3$  represents the most potent catalyst for converting LA, while Cu/ $\text{Al}_2\text{O}_3$  exhibited exceptional selectivity, achieving a 75% MTHF yield after 24 h of reaction time (Table 1, entries 15 and 16). The study also explored the synergetic effects of bimetallic Ni-Cu/ $\text{Al}_2\text{O}_3$  catalysts, revealing a 56% MTHF yield in just 5 h at 250 °C under optimal Ni/Cu ratio conditions (Table 1, entry 17). These bimetallic catalysts demonstrated superior activity and selectivity, attributed to the formation of mixed Ni-Cu particles, which played a pivotal role in enhancing catalytic activity and ultimately improving the desired product's yield.

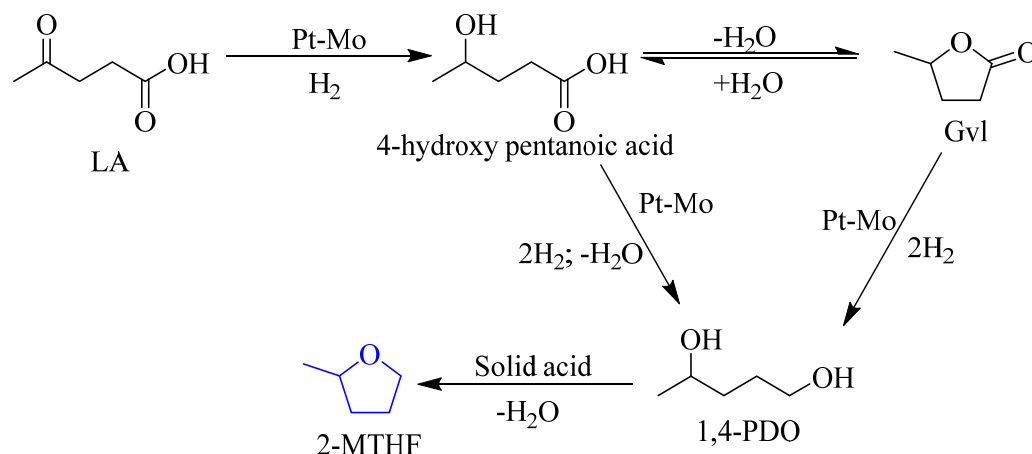
Patankar and Yadav showed the hydrocyclization of LA into Gvl, 1,4-PDO, and 2-MTHF utilizing a Pd-Cu/ $\text{ZrO}_2$  catalyst in an aqueous environment, employing relatively mild reaction conditions (200 °C, 60 bar  $\text{H}_2$ ). Nonetheless, the catalyst exhibited notably low selectivity for 2-MTHF (Table 1, entry 18) [98]. In the case of the mono-metal catalytic system (Cu/ $\text{ZrO}_2$ ) authors observed leaching. This leaching was effectively prevented by adding palladium to the Cu/ $\text{ZrO}_2$  catalyst, forming a stable copper-palladium alloy. The resulting Pd-Cu/ $\text{ZrO}_2$  catalyst demonstrated robustness and stability at high temperatures and pressures. The impact of different supports was investigated in this work using Pd-Cu/HT, Pd-Cu/ $\text{Al}_2\text{O}_3$ , and Pd-Cu/HMS catalysts (Table 1, entries 19 to 21). However, successful cascade synthesis to produce PDO and 2-MTHF from LA was accomplished using the Pd-Cu/ $\text{ZrO}_2$  catalyst due to its larger pore size and acidity, enabling the desired conversions. The authors clearly explained the role of metal sites and acidic sites of support in the effective formation of 2-MTHF (Scheme 5).



**Scheme 5.** Synthesis Mechanism of Gvl, 1,4-PDO, and 2-MTHF from LA using a Pd-Cu/ZrO<sub>2</sub> Catalyst. Scheme adopted from [98].

Kaneda research group demonstrated the preparation of 2-MTHF from LA, efficiently facilitated in a one-pot process using a Pt-Mo bimetallic catalyst supported on H- $\beta$ -zeolite, all in the presence of water and without any additional additives [99]. This catalyst system enables the hydrogenation of levulinic acid into 1,4-PDO, which is subsequently dehydrated to yield 2-MTHF by the H- $\beta$  zeolite in an aqueous environment. The catalyst showed >99% conversion of LA with 86% of 2-MTHF under mild reaction condition i.e., 130 °C, 50 bar H<sub>2</sub> (Table 1, entry 22). The reusability of catalysts is indeed crucial in the chemical industry, especially when working with precious metal catalysts. Precious metals, such as Pt, Pd, Rh, and others, are often used as catalysts in various industrial processes due to their high catalytic activity and selectivity. However, these metals are expensive, making it

economically advantageous to recover and reuse them in multiple reaction cycles. In this work, the catalyst (Pt–Mo/H- $\beta$ ) was recovered and reused for the next two cycles. It showed remarkable activity and maintained the conversion of LA and selectivity of 2-MTHF, similar to the fresh catalyst (Table 1, entries 23 and 24). As per the experimental results, the authors declared that the catalyst support, such as H- $\beta$  serves a dual function. First, it acts as a distinctive solid acid catalyst, facilitating the cyclodehydration of 1,4-pentanediol to 2-methyltetrahydrofuran in a water environment. Second, it functions as a support, enabling a synergistic interaction between Pt nanoparticles and MoO<sub>x</sub> species (Scheme 6). This synergy efficiently promotes the hydrogenation of levulinic acid to 1,4-pentanediol.

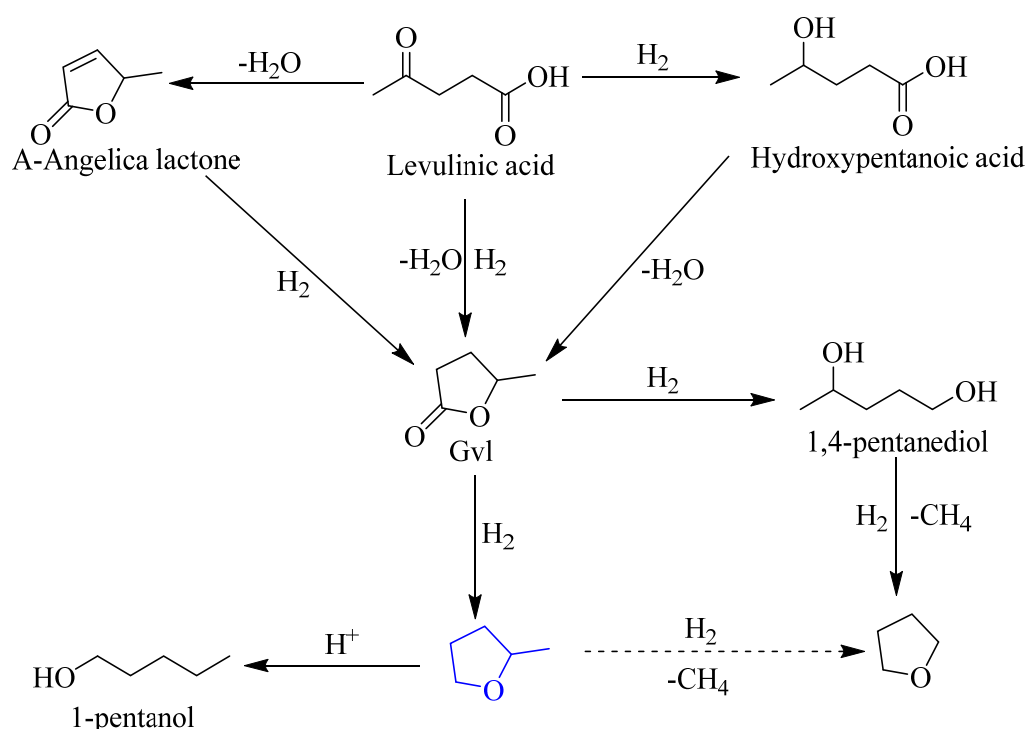


**Scheme 6.** One-pot transformation of LA to 2-MTHF over Pt–Mo/H- $\beta$ . Scheme adopted from [99].

Upare et al. reported graphene oxide (GO) supported ruthenium nanoparticles (Ru/GO) for the hydrogenation of LA to produce cyclic ethers in a fixed-bed reactor (vapor-phase) [100]. Remarkably, Ru/GO catalysts exhibited a diverse range of hydrogenation products, including cyclic ethers (2-THF and tetrahydrofuran-THF at 54%) and Gvl at 41%. In order to increase the production of cyclic ethers, a two-step hydrogenation procedure was effectively employed to convert LA to Gvl. This method involved using Gvl as a secondary feedstock, enabling Ru/GO catalysts to generate cyclic ethers, including 2-MTHF and THF. The Ru/GO catalysts displayed exceptional selectivity, with an impressive 92% preference for cyclic ethers, notably achieving 77% selectivity for 2-MTHF, as evidenced in the two-step process (Table 1, entry 25). The outstanding activity and selectivity of LA hydrogenation over Ru/GO were attributed to the well-dispersed Ru nanoparticles and favorable interactions with GO, facilitated by the presence of oxy-functional groups (–carboxyl, –epoxy, –hydroxyl, etc.) on GO. Gvl was unequivocally established as the primary intermediate in 2-MTHF synthesis from LA, and there are two prominent routes for MTHF production from Gvl. The first step entails the hydrogenation of LA’s carbonyl group to produce Gvl on metallic catalyst sites. The second step involves the hydrogenation of Gvl to 1,4-PDO, also on metallic catalyst sites, followed by dehydration to form 2-MTHF with the assistance of acidic sites (Scheme 7). Under reduced hydrogen pressure, the major product obtained with Ru/GO catalysts was 1,4-PDO instead of 2-MTHF. Conversely, increasing the hydrogen pressure facilitated the formation of 2-MTHF, with 1,4-PDO acting as an intermediate (Table 1, entries 26 and 27).

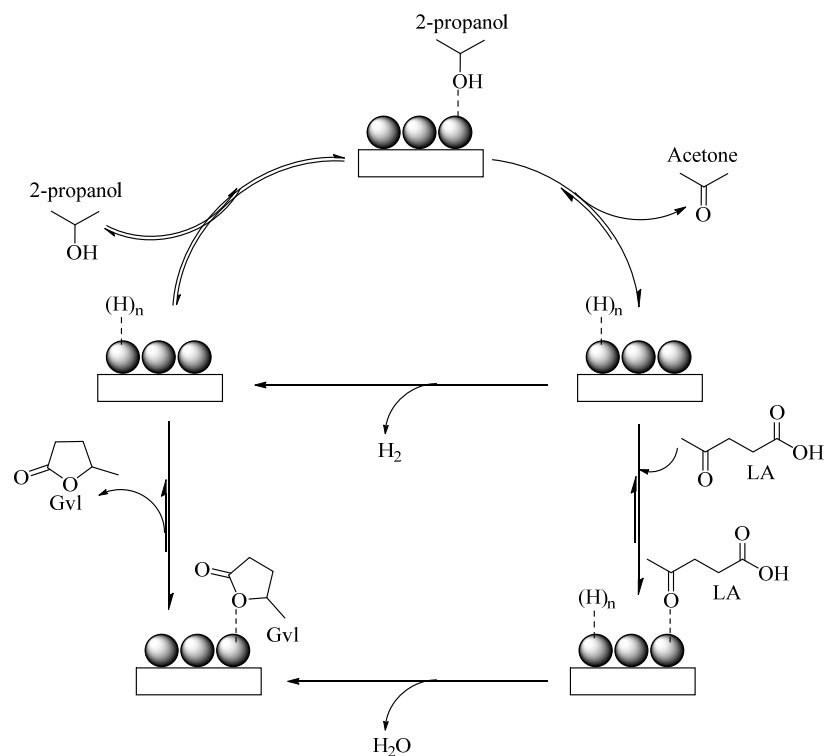
Obregon et al. investigated two potential sources of hydrogen, molecular H<sub>2</sub> (catalytic hydrogenation) and alcohols (catalytic transfer hydrogenation-CTH), for the transformation of LA to 2-MTHF over Ni–Cu/Al<sub>2</sub>O<sub>3</sub> catalysts [50]. While individual hydrogenation through either CTH or molecular H<sub>2</sub> alone yielded Gvl (80–90%) in amounts ranging, the production of MTHF was minimal (less than 3%) under moderate reaction conditions (5 h, 40 bar H<sub>2</sub>, 250 °C). However, under these reaction conditions, combining both hydrogen sources was essential to achieve a substantial yield of 2-MTHF (40%) (Table 1, entry 28). Indeed, it was observed that the presence of molecular H<sub>2</sub> pressure had a beneficial effect

on the reaction. This increased the concentration of dissolved hydrogen in the reaction medium, thereby decreasing hydrogen desorption from the catalyst surface. This increased availability of hydrogen greatly facilitated the efficient conversion of Gvl, resulting in a notable yield of MTHF. Additionally, the study established a direct correlation between the results in nitrogen ( $N_2$ ) and hydrogen ( $H_2$ ) atmospheres, underscoring the crucial role of catalytic hydrogenation in the conversion of LA to MTHF, even under high  $H_2$  pressure (Schemes 8 and 9). In the  $N_2$  atmospheric reaction case, only a trace amount of 2-MTHF is observed, and in the  $H_2$  atmospheric case, a moderate yield of 2-MTHF was observed. The hydrogen pressure amplifies the amount of dissolved  $H_2$  in the reaction medium. This increase facilitates the adsorption of hydrogen atoms while reducing their desorption rate, which is not observed in the case of  $N_2$  atmosphere (Table 1, entry 28 and 29). In summary of this work, employing Ni-Cu/ $Al_2O_3$  catalyst in conjunction with a proficient hydrogen donor solvent (2-propanol), and operating under an  $H_2$  atmosphere, yielded impressive 2-MTHF rates of up to 80% after a 20 h reaction period (Table 1, entry 30).

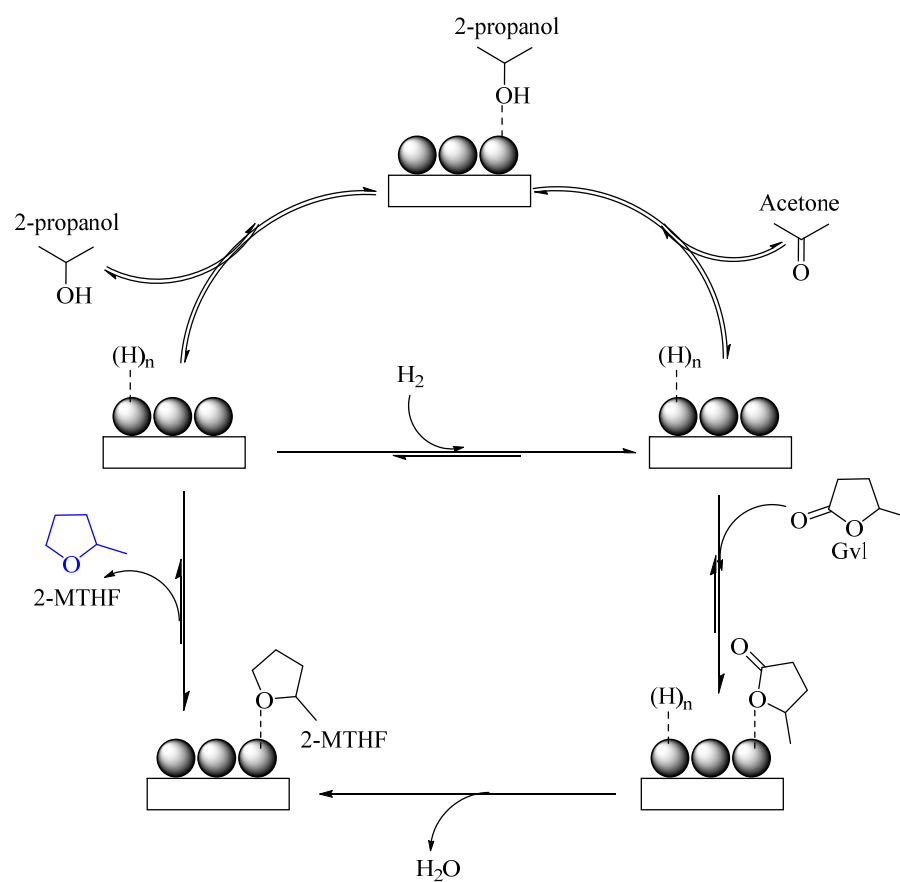


**Scheme 7.** Reaction network of LA to tetrahydrofuranic compounds using Ru/GO catalyst. Scheme adopted from [100].

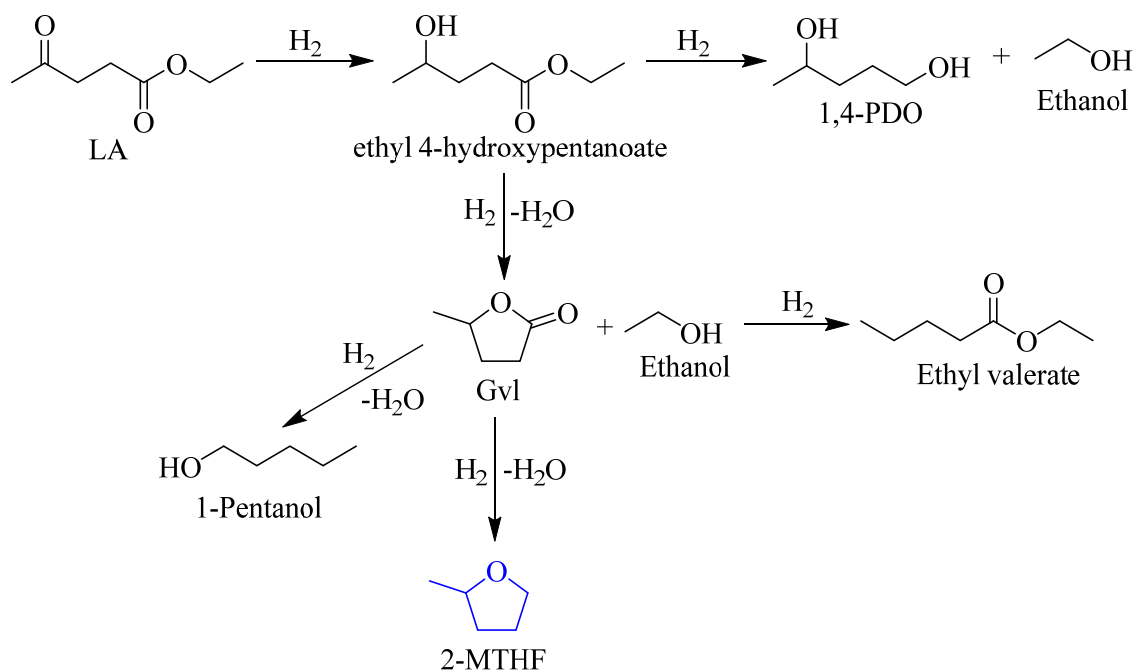
Zheng et al. investigated the effect of reaction temperature on the hydro-conversion of ethyl levulinate (EL) under continuous reaction conditions using Cu/ $Al_2O_3$ - $SiO_2$  catalyst [101]. At 140 °C, only 79% of EL was converted, with an impressive Gvl selectivity of 96%, and no quantity of 2-MTHF is observed at this temperature (Table 1, entry 31). Increasing the temperature to 150 °C enhanced EL conversion to 98% and remained the Gvl selectivity with a minimal 0.25% formation of 2-MTHF, and at 200 °C, 2-MTHF was observed with 9% selectivity (Table 1, entries 32 and 33). At lower reaction temperatures, effectively suppress the formation of undesired byproducts such as ring opened products (pentanol, pentanediol, ethyl pentanoate, etc.) (Scheme 10). However, with a stepwise increase in temperature, significant changes in selectivity were observed. The selectivity towards 2-MTHF increased at the expense of Gvl. At temperatures as high as 250 °C, 2-MTHF became the primary product, with 65% selectivity (Table 1, entry 34). At this temperature, the selectivity of Gvl is reduced to 8%, and the selectivity for 1-pentanol and ethyl valerate reached 17% and 4%, respectively.



**Scheme 8.** Catalytic transfer hydrogenation of LA in the presence of  $N_2$  atmosphere. Scheme adopted from [50].



**Scheme 9.** Catalytic transfer hydrogenation of LA in the presence of  $H_2$  atmosphere. Scheme adopted from [50].

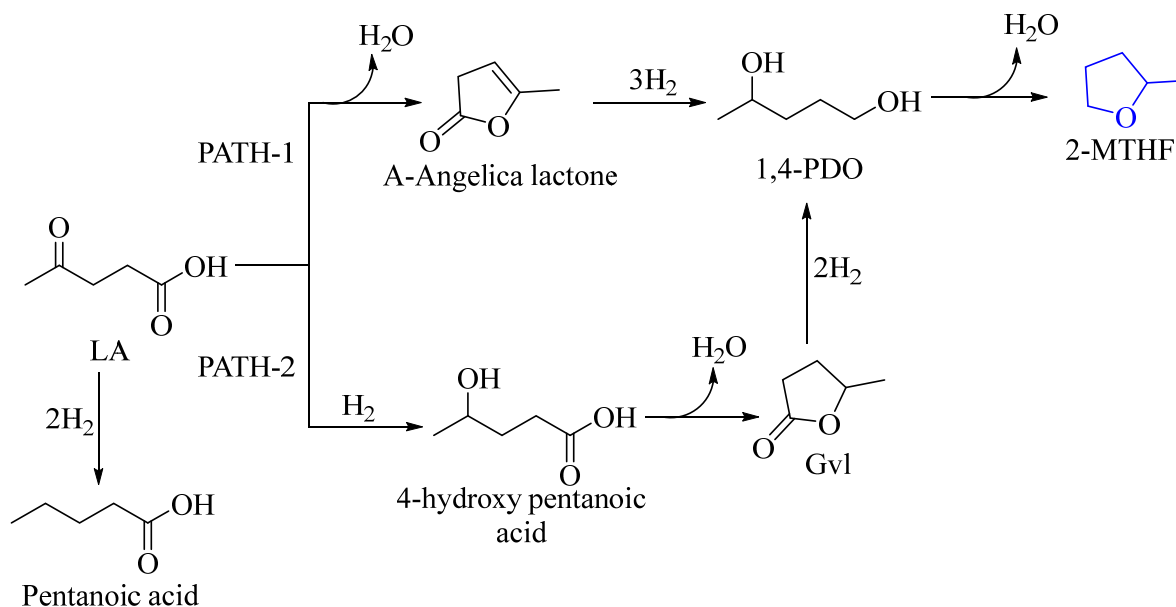


**Scheme 10.** Hydro-conversion of Ethyl levulinate to 2-MTHF. Scheme adopted from [101].

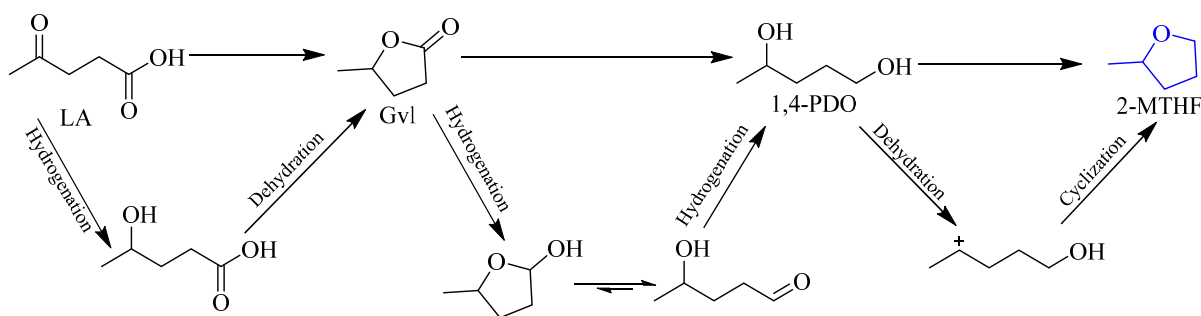
Galletti and team explored the application of carbon-supported ruthenium (Ru) and rhenium (Re) metal catalysts in conjunction with niobium phosphate as an acid co-catalyst. This approach was devised to enhance selectivity in generating 2-MTHF from LA and Gvl [102]. In this research, the integration of a commercially available rhenium-based catalyst (10% Re/C) into an established catalytic system comprising Ru/C and NBP was examined. When employed independently, the Re/C catalyst showed no activity in the hydroconversion of Gvl. Nevertheless, in conjunction with [Ru/C + NBP], the Re/C catalyst demonstrated a synergistic effect, amplifying both Gvl conversion and selectivity towards 2-MTHF (Table 1, Entry 35). This synergy was observed even at low Re/C concentrations, highlighting the crucial role of rhenium in promoting the cyclization of diols to 2-MTHF in the reaction. The acidity of the co-catalyst (NBP) played a significant role in transforming LA and Gvl into 2-MTHF. The acidic nature of the co-catalyst facilitated interaction with Gvl's carboxylic group, leading to its ring opening and subsequent conversion. Furthermore, the introduction of an acid co-catalyst (NBP) into [Ru/C + Re/C] systems was explored due to its known ability to activate not only lactone ring opening but also the internal dehydration of 1,4-PDO (intermediate in the reaction) to 2-MTHF (Scheme 11). The same catalyst was also employed for the hydroconversion of LA to 2-MTHF, resulting in 100% conversion of LA with 28% selectivity towards 2-MTHF (Table 1, Entry 36). The stepwise reactions, such as hydrogenation and dehydration occurring during the conversion of LA to 2-MTHF using functional catalysts (metal on acidic supports), are depicted in Scheme 12.

Mihályi research group studied solvent-free hydroconversion of LA using Co/SiO<sub>2</sub> catalyst in a continuous process using a fixed-bed microreactor [103]. The catalyst is a bifunctional catalyst that consists of Co metal (for hydrogenation/hydrogenolysis reaction) and CoO<sub>x</sub> Lewis acid active sites (dehydration reaction). During the reaction, the LA was initially dehydrated to create an angelica lactone (AL) intermediate. The selectivity of the reaction was influenced by the hydrogenation/hydrogenolysis activity of the catalyst, given the ease of LA dehydration. Under steady-state conditions at 200 °C and 30 bar pressure, the catalyst solely saturated the double bond of the AL ring, resulting in a 98 mol% yield of Gvl at complete LA conversion. However, at 225 °C, the catalyst's high hydrogenation activity led to the cleavage of the Gvl ring, yielding 2-MTHF with a stable yield of approximately 70 mol% (Table 1, entry 37 and 38). These findings indicate that at 200 °C, the reaction produces a catalyst surface that is both active and enduring in selectively generating Gvl

from LA. However, the delicate equilibrium between hydrogenation and dehydration activities, which accounts for the high Gvl selectivity, becomes precarious. With a slight increase in temperature, the heightened hydrogenation activity transforms Gvl into 2-MTHF. FT-IR spectroscopic analysis of adsorbed LA indicated the formation of H-bound LA and surface carboxylates. Surface intermediates, such as 4-hydroxy-3-pentenoate and 4-hydroxypentanoate, were identified during Gvl formation through dehydration.



**Scheme 11.** Conversion of LA to 2-MTHF using Ru/C + Re/C + NBP multi-catalytic system. Scheme adopted from [102].



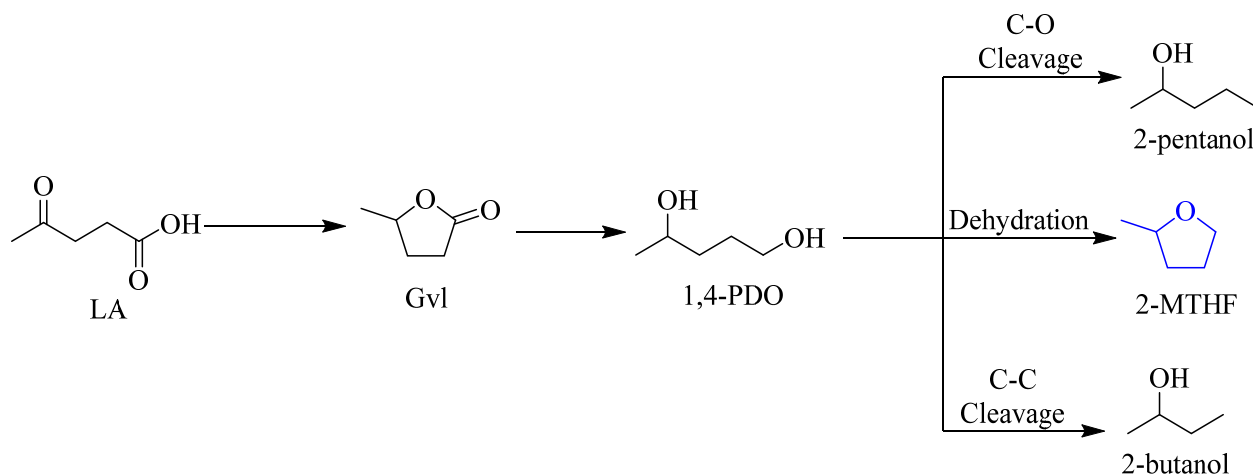
**Scheme 12.** Stepwise reactions (hydrogenation and dehydration) during the conversion of LA to 2-MTHF using functional catalysts (Metal on acidic supports). Scheme adopted from [102].

Xie et al. screened several metal catalysts for this conversion under batch reaction conditions (220 °C, 30 bar H<sub>2</sub>, 10 h) in the presence of 2-butanol medium [104]. The Pd/C and Pt/C catalysts showed selectivity towards Gvl, the Ru/C gave good selectivity towards sec-butyl 4-oxopentanoate and in this case 2-MTHF was observed only 2%. The three above-mentioned catalysts have less selectivity for 2-MTHF. The mesoporous bifunctional and bimetallic such as Cu-Ni/Al<sub>2</sub>O<sub>3</sub>-ZrO<sub>2</sub> (prepared from impregnation technique) exhibited excellent catalytic activity towards selective formation of 2-MTHF (92%) (Table 1, entries 39 to 42). The authors concluded that this exceptional catalytic performance by various physicochemical techniques can be attributed to the catalyst's mesoporous structure, the acidic properties of the support, and the synergistic effects between Cu and Ni. Moreover, the Ni-Cu/Al<sub>2</sub>O<sub>3</sub>-ZrO<sub>2</sub> catalyst demonstrated remarkable stability, retaining its catalytic activity and selectivity even after five reuse cycles. At optimal metal and support ratios, such as Cu (10 wt%)-Ni (10 wt%)/Al<sub>2</sub>O<sub>3</sub>-ZrO<sub>2</sub> (9: Mole ratio of Al to Zr), which revealed

complete conversion of LA to 2-MTHF (99.8%). In this work, we also studied the effect of reaction parameters on the reaction using Ni-Cu/Al<sub>2</sub>O<sub>3</sub>-ZrO<sub>2</sub> catalyst, at below 180 °C, and the predominant product was Gvl. With a rise in temperature beyond this point, MTHF selectivity increased, while the Gvl yield notably dropped. Optimal MTHF selectivity (99.8%) was achieved at 220 °C. However, elevating the temperature further decreased MTHF selectivity due to the formation of by-products like sec-butyl valerate. At low hydrogen pressure, Gvl yield is favored, but increasing H<sub>2</sub> pressure led to higher MTHF selectivity at the expense of Gvl selectivity. MTHF selectivity peaked at 99.8% when H<sub>2</sub> pressure exceeded 30 bar H<sub>2</sub> (Table 1, entry 43). A low reaction pressure hampered the ring-opening/cyclodehydration of Gvl into MTHF, resulting in decreased selectivity. Finally, the authors also studied the reusability activity of Ni/Al<sub>2</sub>O<sub>3</sub>-ZrO<sub>2</sub>, the catalyst displayed the ability to be reused up to five times with minimal loss in both catalytic activity and selectivity.

Gu et al. reported NiCo/γ-Al<sub>2</sub>O<sub>3</sub> catalyst for the conversion of LA to 2-MTHF at various reaction parameters [105]. The proportions of Ni and Co in the NiCo/γ-Al<sub>2</sub>O<sub>3</sub> catalyst were examined. Under optimal conditions, the Ni (5 wt%) Co (25 wt%)/γ-Al<sub>2</sub>O<sub>3</sub> catalyst exhibited significant activity, achieving a 73% yield of 2-MTHF (Table 1, entry 44). X-ray Photoelectron Spectroscopy (XPS) analysis revealed a higher presence of metal oxides on bimetallic catalysts, contrasting with reduced metals (M(0)) predominantly found on monometallic counterparts. Additionally, bimetallic catalysts exhibited heightened acidity compared to their monometallic counterparts, and the presence of metal oxide content in bimetallic catalysts could be the reason for the high acidity of the bimetallic catalyst. Actually, the acidity of the catalyst plays an important role in the conversion of LA to 2-MTHF; the appropriate acidic sites/strength in bimetallic Ni-Co/γ-Al<sub>2</sub>O<sub>3</sub> is the main reason for the highest yield of 2-MTHF as per monometallic catalysts (Table 1, entries 44 to 46). The maximum yield of Gvl reached 95% at 190 °C and exhibited a gradual decline with increasing temperatures. Conversely, the yield of 2-MTHF rose from 0.3% at 190 °C to 73% at 240 °C. A slight decrease to 71% in 2-MTHF yield occurred when the temperature was further increased to 250 °C, indicating that elevated temperatures might induce undesired side reactions. At a H<sub>2</sub> pressure of 10 bar, the yield of 2-MTHF was 33%, with Gvl being the primary product at 54%. As the H<sub>2</sub> pressure increased from 10 bar H<sub>2</sub> to 50 bar H<sub>2</sub>, there was a gradual rise in the yield of 2-MTHF, reaching 73% at 50 bar H<sub>2</sub>. However, further increasing the pressure to 60 bar H<sub>2</sub> did not enhance the 2-MTHF yield, indicating a saturation point for the surface M-H (M = Ni and Co) species at 50 bar H<sub>2</sub>. Additionally, there was a gradual increase in the yield of 2-butanol (C-C cleavage of 1,4-PDO intermediate), underscoring the competitive nature between the production of 2-MTHF and monoalcohol (Scheme 13). In the initial hour, a low yield of 2-MTHF at 12% was observed, with Gvl being the primary product at 76%. This indicated an insufficient reaction time for the production of 2-MTHF. With an extended reaction time of 5 h, the 2-MTHF yield increased to 73%, and there was also a rise in the yield of 2-butanol. Further extending the reaction time to 6 h resulted in a slight decrease in 2-MTHF yield (72%), while the yield of 2-butanol increased, which means after 6 h the conversion initiates C-C cleavage to form alcohol products. The authors also investigated reuse of the NiCo/γ-Al<sub>2</sub>O<sub>3</sub> catalyst, four consecutive cycles of LA to 2-MTHF were conducted at 240 °C, 5 bar H<sub>2</sub> for 4 h; there was a slight decrease in the conversion of LA and the yield of 2-MTHF. The comparative yield of 2-MTHF decreased from 66% to 63% over these four runs, with the conversion of LA gradually decreasing from 92% to 87%. This reusability experiment suggests that the NiCo/γ-Al<sub>2</sub>O<sub>3</sub> exhibits promising stability and reusability.

The Seames research group demonstrated the conversion of LA to 2-MTHF in two steps: 1. Catalytic Transfer Hydrogenation (isopropanol as a hydrogen source) of LA to Gvl using Zr containing β-zeolite catalyst, 2. Catalytic hydro-conversion of Gvl (obtained in the first step) to using CuO/Al<sub>2</sub>O<sub>3</sub> catalyst in the presence of a molecular H<sub>2</sub> source at batch and continuous operations [46].



**Scheme 13.** Reaction products of hydro-conversion of LA over NiCo/ $\gamma$ -Al<sub>2</sub>O<sub>3</sub> catalyst. Scheme adopted from [105].

In the first step the Zr- $\beta$ -zeolite catalyst showed 97% selectivity towards the Gvl at relatively milder reaction conditions (Table 1, entry 47).

The optimal conditions for maximizing the conversion of Gvl to 2-MTHF in the second reaction were established as follows:

- In batch reaction conditions, the conversion of Gvl to 2-MTHF shows an 84% yield (96% of sel.) using CuO/Al<sub>2</sub>O<sub>3</sub> catalyst (Table 1, entry 48).
- In fixed-bed reaction conditions (continuous process), the conversion of Gvl to 2-MTHF shows a 93% yield (98% of sel.) using CuO/Al<sub>2</sub>O<sub>3</sub> catalyst (Table 1, entry 49).

The reaction temperature 200 °C showed maximum selectivity towards 2-MTHF; at lower temperatures, the reaction favored the formation of 1,4-PDO, but this effect could be mitigated by extending the residence time. At reaction temperatures of 250 °C or higher led to unwanted side reactions such as ring opening products.

**Table 1.** Catalytic conversion of LA to 2-MTHF.

| S. No | Catalyst  | Reactant | Reaction Conditions (Temp., H <sub>2</sub> Pressure, Time in Hours)                              | Conv. (%) | 2-MTHF sel. (%) | Ref. |
|-------|---|----------|--|-----------|-----------------|------|
| 1     | 5 wt% Cu/Al <sub>2</sub> O <sub>3</sub>                 | LA       | 265 °C, H <sub>2</sub> (10 bar), time (5 h), <i>p</i> -dioxane, fixed-bed reactor (vapour phase) | 100       | 0.1             | [53] |
| 2     | 30 wt% Cu/Al <sub>2</sub> O <sub>3</sub>                | LA       | 265 °C, H <sub>2</sub> (10 bar), time (5 h), <i>p</i> -dioxane, fixed-bed reactor (vapour phase) | 100       | 3               | [53] |
| 3     | 50 wt% Cu/Al <sub>2</sub> O <sub>3</sub>                | LA       | 265 °C, H <sub>2</sub> (10 bar), time (5 h), <i>p</i> -dioxane, fixed-bed reactor (vapour phase) | 100       | 43              | [53] |
| 4     | 80 wt% Cu/Al <sub>2</sub> O <sub>3</sub>                | LA       | 265 °C, H <sub>2</sub> (10 bar), time (5 h), <i>p</i> -dioxane, fixed-bed reactor (vapour phase) | 100       | 64              | [53] |
| 5     | 8 wt% Ni-72 wt% Cu/SiO <sub>2</sub>                     | LA       | 265 °C, H <sub>2</sub> (10 bar), time (5 h), <i>p</i> -dioxane, fixed-bed reactor (vapour phase) | 100       | 89              | [53] |
| 6     | Ru-Starbon®   | LA       | 150 °C, time (30 min), 300 W (microwave irradiation), FA as H <sub>2</sub> source                | 30        | 50              | [96] |
| 7     | Rh-Starbon®   | LA       | 150 °C, time (30 min), 300 W (microwave irradiation), FA as H <sub>2</sub> source                | 69        | 90              | [96] |
| 8     | Pd-Starbon®   | LA       | 150 °C, time (30 min), 300 W (microwave irradiation), FA as H <sub>2</sub> source                | 64        | 88              | [96] |
| 9     | Cu-MINT   | LA       | 150 °C, time (30 min), 300 W (microwave irradiation), FA as H <sub>2</sub> source                | 90        | 75              | [96] |
| 10    | Pd/C  | LA       | 150 °C, time (30 min), 300 W (microwave irradiation), FA as H <sub>2</sub> source                | 78        | 92              | [96] |
| 11    | Ru[H <sub>2</sub> CON(PPh <sub>2</sub> ) <sub>3</sub> ] | LA       | 150 °C, H <sub>2</sub> (65 bar), 25 h, THF, batch reactor  | 100       | 87              | [97] |
| 12    | Ni/Al <sub>2</sub> O <sub>3</sub>                       | LA       | 250 °C, H <sub>2</sub> (70 bar), 5 h, H <sub>2</sub> O, batch reactor                            | 100       | 1.4             | [52] |
| 13    | Ni/Al <sub>2</sub> O <sub>3</sub>                       | LA       | 250 °C, H <sub>2</sub> (70 bar), 5 h, ethanol, batch reactor                                     | 100       | 0.5             | [52] |
| 14    | Ni/Al <sub>2</sub> O <sub>3</sub>                       | LA       | 250 °C, H <sub>2</sub> (70 bar), 5 h, 1-butanol, batch reactor                                   | 93        | 10              | [52] |

Table 1. Cont.

| S. No | Catalyst   | Reactant                   | Reaction Conditions (Temp., H <sub>2</sub> Pressure, Time in Hours)  | Conv. (%) | 2-MTHF sel. (%)              | Ref.  |
|-------|--|----------------------------|--|-----------|------------------------------|-------|
| 15    | Ni/Al <sub>2</sub> O <sub>3</sub>                                      | LA                         | 250 °C, H <sub>2</sub> (70 bar), 5 h, 2-propanol, batch reactor  | 100       | 46                           | [52]  |
| 16    | Cu/Al <sub>2</sub> O <sub>3</sub>                                      | LA                         | 250 °C, H <sub>2</sub> (70 bar), 24 h, 2-propanol, batch reactor   | 100       | 75                           | [52]  |
| 17    | Ni-Cu/Al <sub>2</sub> O <sub>3</sub>                                   | LA                         | 250 °C, H <sub>2</sub> (70 bar), 5 h, 2-propanol, batch reactor  | 100       | 56                           | [52]  |
| 18    | Pd-Cu/ZrO <sub>2</sub>   | LA                         | 200 °C, 50 bar H <sub>2</sub> , 24 h, H <sub>2</sub> O, batch reactor  | 100       | 25% 1,4-PDO<br>5% 2-MTHF     | [98]  |
| 19    | Pd-Cu/HT   | LA                         | 200 °C, 50 bar H <sub>2</sub> , 24 h, H <sub>2</sub> O, batch reactor  | 100       | Not observed                 | [98]  |
| 20    | Pd-Cu/Al <sub>2</sub> O <sub>3</sub>                                   | LA                         | 200 °C, 50 bar H <sub>2</sub> , 24 h, H <sub>2</sub> O, batch reactor  | 100       | Not observed                 | [98]  |
| 21    | Pd-Cu/HMS  | LA                         | 200 °C, 50 bar H <sub>2</sub> , 24 h, H <sub>2</sub> O, batch reactor  | 100       | Not observed                 | [98]  |
| 22    | Pt–Mo/H-β  | LA                         | 150 °C, 50 bar H <sub>2</sub> , 12 h, H <sub>2</sub> O, batch reactor  | >99       | 86                           | [99]  |
| 23    | Pt–Mo/H-β<br>(reused—1st Cycle)  | LA                         | 150 °C, 50 bar H <sub>2</sub> , 12 h, H <sub>2</sub> O, batch reactor  | >99       | 85                           | [99]  |
| 24    | Pt–Mo/H-β<br>(reused—2nd Cycle)  | LA                         | 150 °C, 50 bar H <sub>2</sub> , 12 h, H <sub>2</sub> O, batch reactor  | >99       | 85                           | [99]  |
| 25    | 5% Ru/GO   | Gvl (obtained from LA)     | 265 °C, 25 bar H <sub>2</sub> , 1,4-dioxane in fixed-bed reactor   | 100       | 92% (77% 2-MTHF and 15% THF) | [100] |
| 26    | 5% Ru/GO   | Gvl (obtained from LA)     | 265 °C, 10 bar H <sub>2</sub> , 1,4-dioxane in fixed-bed reactor   | 69        | 83% PDO                      | [100] |
| 27    | 5% Ru/GO   | Gvl (obtained from LA)     | 265 °C, 1 bar H <sub>2</sub> , 1,4-dioxane in fixed-bed reactor  | 48        | 92% PDO                      | [100] |
| 28    | Ni-Cu/Al <sub>2</sub> O <sub>3</sub>                                   | LA                         | 250 °C, 40 bar H <sub>2</sub> , 5 h, 2-Propanol, batch reactor   | 100       | 40                           | [50]  |
| 29    | Ni-Cu/Al <sub>2</sub> O <sub>3</sub>                                   | LA                         | 250 °C, 40 bar N <sub>2</sub> , 5 h, 2-Propanol, batch reactor   | 100       | <5                           | [50]  |
| 30    | Ni-Cu/Al <sub>2</sub> O <sub>3</sub>                                   | LA                         | 250 °C, 40 bar H <sub>2</sub> , 20 h, 2-Propanol, batch reactor  | 100       | 80                           | [50]  |
| 31    | Cu/Al <sub>2</sub> O <sub>3</sub> -SiO <sub>2</sub>                    | EL                         | 140 °C, 15 bar H <sub>2</sub> , ethanol, fixed-bed reactor   | 79        | Nil                          | [101] |
| 32    | Cu/Al <sub>2</sub> O <sub>3</sub> -SiO <sub>2</sub>                    | EL                         | 150 °C, 15 bar H <sub>2</sub> , ethanol, fixed-bed reactor   | 98        | 0.25                         | [101] |
| 33    | Cu/Al <sub>2</sub> O <sub>3</sub> -SiO <sub>2</sub>                    | EL                         | 200 °C, 15 bar H <sub>2</sub> , ethanol, fixed-bed reactor   | 99        | 9                            | [101] |
| 34    | Cu/Al <sub>2</sub> O <sub>3</sub> -SiO <sub>2</sub>                    | EL                         | 250 °C, 15 bar H <sub>2</sub> , ethanol, fixed-bed reactor   | 100       | 65                           | [101] |
| 35    | Ru/C + Re/C + NBP  | Gvl                        | 200 °C, 90 bar H <sub>2</sub> , 3 h, H <sub>2</sub> O, batch reactor   | 40        | 65                           | [102] |
| 36    | Ru/C + Re/C + NBP  | LA                         | 180 C, 50 bar H <sub>2</sub> , 3 h, H <sub>2</sub> O, batch reactor  | 100       | 28                           | [102] |
| 37    | Co/SiO <sub>2</sub>  | LA                         | 200 °C, 30 bar H <sub>2</sub> , No solvent, fixed-bed reactor  | 100       | trace                        | [103] |
| 38    | Co/SiO <sub>2</sub>  | LA                         | 225 °C, 30 bar H <sub>2</sub> , No solvent, fixed-bed reactor  | 100       | 70                           | [103] |
| 39    | 5% Pd/C  | LA                         | 220 °C, 30 bar H <sub>2</sub> , 10 h, 2-butanol, batch reactor   | 100       | 6.4                          | [104] |
| 40    | 5% Pt/C  | LA                         | 220 °C, 30 bar H <sub>2</sub> , 10 h, 2-butanol, batch reactor   | 100       | 10                           | [104] |
| 41    | 5% Ru/C  | LA                         | 220 °C, 30 bar H <sub>2</sub> , 10 h, 2-butanol, batch reactor   | 100       | 2.6                          | [104] |
| 42    | Cu (5%)-Ni (10%)/Al <sub>2</sub> O <sub>3</sub> -ZrO <sub>2</sub> (9)  | LA                         | 220 °C, 30 bar H <sub>2</sub> , 10 h, 2-butanol, batch reactor   | 100       | 92.3                         | [104] |
| 43    | Cu (10%)-Ni (10%)/Al <sub>2</sub> O <sub>3</sub> -ZrO <sub>2</sub> (9) | LA                         | 220 °C, 30 bar H <sub>2</sub> , 10 h, 2-butanol, batch reactor   | 100       | 99.8                         | [104] |
| 44    | Ni-Co/γ-Al <sub>2</sub> O <sub>3</sub>                                 | LA                         | 250 °C, H <sub>2</sub> (50 bar), 5 h, isopropanol, batch reactor   | 99.9      | 73                           | [105] |
| 45    | Co/γ-Al <sub>2</sub> O <sub>3</sub>                                    | LA                         | 250 °C, H <sub>2</sub> (50 bar), 5 h, isopropanol, batch reactor   | 99.9      | 62                           | [105] |
| 46    | Ni/γ-Al <sub>2</sub> O <sub>3</sub>                                    | LA                         | 250 °C, H <sub>2</sub> (50 bar), 5 h, isopropanol, batch reactor   | 99.9      | 17                           | [105] |
| 47    | Zr-β-zeolite   | LA                         | 170 °C, H <sub>2</sub> (50 bar), 4 h, isopropanol, batch reactor   | -         | 97 (88% yield) *             | [46]  |
| 48    | CuO/Al <sub>2</sub> O <sub>3</sub>                                     | Gvl (obtained in 1st step) | 200 °C, H <sub>2</sub> (15 bar), 2 h, batch reactor  | -         | 96 (84% yield)               | [46]  |
| 49    | CuO/Al <sub>2</sub> O <sub>3</sub>                                     | Gvl (obtained in 1st step) | 200 °C, time (residence) of 2.5 h, and a feed rate 10 mol% excess H <sub>2</sub> , 2-propanol, fixed-bed reactor | -         | 98 (93% yield)               | [46]  |

\* Yield and selectivity of Gvl.

#### 4. Conclusions and Outlook

Synthesizing 2-methyltetrahydrofuran (2-MTHF) from levulinic acid (LA) presents a major challenge in bio-refinery processes. The significance of 2-MTHF in biofuel and its safe solvent applications in diverse industries has led to extensive research efforts to address this challenge. In batch reactions, the Pt–Mo/H-β catalyst demonstrated high efficiency, yielding 2-MTHF at an 85–86% rate from LA in an aqueous medium at 150 °C,

the H- $\beta$  support acidity in promoting synergistic interactions between Pt nanoparticles and MoO<sub>x</sub> species were key findings. Another, i.e., Cu-Ni/Al<sub>2</sub>O<sub>3</sub>-ZrO<sub>2</sub>, with equivalent Cu-10 wt% and Ni-10 wt% on ZrO<sub>2</sub> support, achieved the highest catalytic activity, yielding 99% of 2-MTHF in the presence of 2-butanol. Its exceptional performance was attributed to the acidic characteristics of the support and the synergistic interactions between Cu and Ni. The CuO/Al<sub>2</sub>O<sub>3</sub> catalyst precursor yielded 85% 2-MTHF from Gvl at 200 °C, 15 bar H<sub>2</sub> pressure, and 2 h. Similarly, the Ni-Cu/Al<sub>2</sub>O<sub>3</sub> catalyst achieved an 80% yield of 2-MTHF from LA using molecular hydrogen and 2-butanol as hydrogen sources, with both sources enhancing selectivity towards 2-MTHF. The Ni-Co/ $\gamma$ -Al<sub>2</sub>O<sub>3</sub> catalyst proved to be a highly effective bimetallic catalyst, achieving a 73% yield of 2-MTHF from LA and emphasizing the significance of suitable acidic sites. Under microwave irradiation, Rh-Starbon<sup>®</sup>, Pd-Starbon<sup>®</sup>, Cu-MINT, and Pd/C catalysts yielded 2-MTHF with selectivity ranging from 75% to 95% and moderate LA conversion.

In fixed-bed conditions, a high metal content catalytic system (8 wt% Ni and 72 wt% Cu on SiO<sub>2</sub>) achieved an excellent yield (89%) of 2-MTHF at 265 °C and 25 bar H<sub>2</sub> pressure in a 1,4-dioxane medium, marking the first report of such a high yield under these conditions. Similarly, the copper-based catalyst Cu/Al<sub>2</sub>O<sub>3</sub>-SiO<sub>2</sub> showed a substantial 65% yield of 2-MTHF from ethyl levulinate in an ethanol medium under comparable reaction conditions. A non-noble metal catalyst, Co/SiO<sub>2</sub>, demonstrated complete LA conversion with a remarkable 70% selectivity towards 2-MTHF under solvent-free conditions. Additionally, the Ru/GO catalyst exhibited a high yield of tetrahydrofurans (77% 2-MTHF and 15% THF) from LA at 265 °C and 25 bar H<sub>2</sub> pressure in the presence of a 1,4-dioxane medium. This success was attributed to well-dispersed Ru nanoparticles and their favorable interactions with the graphene oxide (GO) support, facilitated by the presence of oxygen-functional groups, enhancing the catalytic activity of Ru/GO.

Several noteworthy aspects are involved in the transformation of LA into 2-MTHF. The introduction of co-metal to the catalyst enhances the selectivity of 2-MTHF, as exemplified by the utilization of Ni metal in the vapor phase with Cu/SiO<sub>2</sub>. The remarkable activity and selectivity demonstrated by catalysts in producing 2-MTHF can be credited to well-dispersed metal nanoparticles and favorable interactions facilitated by oxygen-functional groups (-carboxyl, -epoxy, -hydroxyl, etc.) on the support. This phenomenon is evident in the case of Ru/GO. An alcohol-based hydrogen source, such as 2-propanol, emerged as the most efficient solvent in the reaction, generating H<sub>2</sub> through decomposition. The hydrogen produced was then employed in the conversion of LA to 2-MTHF. The Ni-Cu-supported catalyst exhibited remarkable catalytic activity for this conversion in the presence of 2-propanol. Temperature plays a pivotal role in LA conversion, with the range of 170–240 °C being conducive to 2-MTHF formation, while elevated temperatures result in the generation of ring-opening products. The pressure of hydrogen is a critical factor, as lower pressures promote Gvl yield, whereas higher pressures boost 2-MTHF selectivity. Bimetallic catalysts, characterized by heightened acidity attributed to metal oxides, exert a significant influence on the conversion of LA to 2-MTHF.

The conversion process faces challenges because of the use of hazardous solvents, excessive metal content in catalysts, limited selectivity of some catalysts for 2-MTHF, instability of catalytic materials, and low productivity of 2-MTHF. To overcome these problems, there is a need for a catalytic system that works in safer conditions and provides higher yields and throughput of 2-MTHF, all under relatively moderate reaction conditions. Tackling these challenges is a crucial and ambitious goal in bio-refinery research.

**Author Contributions:** S.G. and S.K.K. made equal contributions to conceptualization, original draft preparation, review, and editing. All authors have read and agreed to the published version of the manuscript.

**Funding:** This research received no external funding.

**Institutional Review Board Statement:** Not applicable.

**Informed Consent Statement:** Not applicable.

**Data Availability Statement:** Not applicable.

**Acknowledgments:** The authors express gratitude to the Koneru Lakshmaiah Education Foundation (KL Deemed to be University) and The Odisha Renewable Energy Research Institute (ORERI) for their support.

**Conflicts of Interest:** The authors declare no conflict of interest.

## References

1. Romashov, L.V.; Kucherov, F.A.; Kozlov, K.S.; Ananikov, V.P. Bio-Derived Furanic Compounds with Natural Metabolism: New Sustainable Possibilities for Selective Organic Synthesis. *Int. J. Mol. Sci.* **2023**, *24*, 3997. [[CrossRef](#)] [[PubMed](#)]
2. He, J.; Qiang, Q.; Liu, S.; Song, K.; Zhou, X.; Guo, J.; Zhang, B.; Li, C. Upgrading of biomass-derived furanic compounds into high-quality fuels involving aldol condensation strategy. *Fuel* **2021**, *306*, 121765. [[CrossRef](#)]
3. Liu, B.; Zhang, Z. One-Pot Conversion of Carbohydrates into Furan Derivatives via Furfural and 5-Hydroxymethylfurfural as Intermediates. *ChemSusChem* **2016**, *9*, 2015–2036. [[CrossRef](#)] [[PubMed](#)]
4. Takkellapati, S.; Li, T.; Gonzalez, M.A. An overview of biorefinery-derived platform chemicals from a cellulose and hemicellulose biorefinery. *Clean Technol. Environ. Policy* **2018**, *20*, 1615–1630. [[CrossRef](#)] [[PubMed](#)]
5. Karupphasamy, K.; Theerthagiri, J.; Selvaraj, A.; Vikraman, D.; Parangusan, H.; Mythili, R.; Choi, M.Y.; Kim, H.-S. Current trends and prospects in catalytic upgrading of lignocellulosic biomass feedstock into ultrapure biofuels. *Environ. Res.* **2023**, *226*, 115660. [[CrossRef](#)] [[PubMed](#)]
6. Deng, W.; Feng, Y.; Fu, J.; Guo, H.; Guo, Y.; Han, B.; Jiang, Z.; Kong, L.; Li, C.; Liu, H.; et al. Catalytic conversion of lignocellulosic biomass into chemicals and fuels. *Green Energy Environ.* **2023**, *8*, 10–114. [[CrossRef](#)]
7. Liu, X.; Yu, D.; Luo, H.; Li, C.; Li, H. Efficient Reaction Systems for Lignocellulosic Biomass Conversion to Furan Derivatives: A Minireview. *Polymers* **2022**, *14*, 3671. [[CrossRef](#)] [[PubMed](#)]
8. Ahmad, F.B.; Kalam, M.A.; Zhang, Z.; Masjuki, H.H. Sustainable production of furan-based oxygenated fuel additives from pentose-rich biomass residues. *Energy Convers. Manag. X* **2022**, *14*, 100222. [[CrossRef](#)]
9. Kucherov, F.A.; Romashov, L.V.; Galkin, K.I.; Ananikov, V.P. Chemical Transformations of Biomass-Derived C6-Furanic Platform Chemicals for Sustainable Energy Research, Materials Science, and Synthetic Building Blocks. *ACS Sustain. Chem. Eng.* **2018**, *6*, 8064–8092. [[CrossRef](#)]
10. Solarte-Toro, J.C.; Ortiz-Sanchez, M.; Inocencio-García, P.-J.; Cardona Alzate, C.A. Sustainable Biorefineries Based on Catalytic Biomass Conversion: A Review. *Catalysts* **2023**, *13*, 902. [[CrossRef](#)]
11. Jiang, Z.; Zeng, Y.; Hu, D.; Guo, R.; Yan, K.; Luque, R. Chemical transformations of 5-hydroxymethylfurfural into highly added value products: Present and future. *Green Chem.* **2023**, *25*, 871–892. [[CrossRef](#)]
12. Adhami, W.; Richel, A.; Len, C. A review of recent advances in the production of furfural in batch system. *Mol. Catal.* **2023**, *545*, 113178. [[CrossRef](#)]
13. Trapasso, G.; Mazzi, G.; Chicharo, B.; Annatelli, M.; Dalla Torre, D.; Aricò, F. Multigram Synthesis of Pure HMF and BHMF. *Org. Process Res. Dev.* **2022**, *26*, 2830–2838. [[CrossRef](#)] [[PubMed](#)]
14. Aranha, D.J.; Gogate, P.R. A Review on Green and Efficient Synthesis of 5-Hydroxymethylfurfural (HMF) and 2,5-Furandicarboxylic Acid (FDCA) from Sustainable Biomass. *Ind. Eng. Chem. Res.* **2023**, *62*, 3053–3078. [[CrossRef](#)]
15. Jiang, Z.; Hu, D.; Zhao, Z.; Yi, Z.; Chen, Z.; Yan, K. Mini-Review on the Synthesis of Furfural and Levulinic Acid from Lignocellulosic Biomass. *Processes* **2021**, *9*, 1234. [[CrossRef](#)]
16. Zhao, Y.; Lu, K.; Xu, H.; Zhu, L.; Wang, S. A critical review of recent advances in the production of furfural and 5-hydroxymethylfurfural from lignocellulosic biomass through homogeneous catalytic hydrothermal conversion. *Renew. Sustain. Energy Rev.* **2021**, *139*, 110706. [[CrossRef](#)]
17. Xu, C.; Paone, E.; Rodríguez-Padrón, D.; Luque, R.; Mauriello, F. Recent catalytic routes for the preparation and the upgrading of biomass derived furfural and 5-hydroxymethylfurfural. *Chem. Soc. Rev.* **2020**, *49*, 4273–4306. [[CrossRef](#)]
18. Bazoti, S.F.; Bonatto, C.; Scapini, T.; Camargo, A.F.; Treichel, H.; de Oliveira, D. Recent advances, perspectives and challenges on levulinic acid production from residual biomass. *Biofuels Bioprod. Biorefin.* **2023**, *17*, 1068–1084. [[CrossRef](#)]
19. Antonetti, C.; Licursi, D.; Fulignati, S.; Valentini, G.; Galletti, A.M.R. New Frontiers in the Catalytic Synthesis of Levulinic Acid: From Sugars to Raw and Waste Biomass as Starting Feedstock. *Catalysts* **2016**, *6*, 196. [[CrossRef](#)]
20. Gundekari, S.; Kalusulingam, R.; Dakhara, B.; Mani, M.; Mitra, J.; Srinivasan, K. Levulinic Acid- and Furan-Based Multifunctional Materials: Opportunities and Challenges. In *Catalysis for Clean Energy and Environmental Sustainability: Biomass Conversion and Green Chemistry*; Pant, K.K., Gupta, S.K., Ahmad, E., Eds.; Springer International Publishing: Cham, Switzerland, 2021; Volume 1, pp. 291–343.
21. Liu, C.; Lu, X.; Yu, Z.; Xiong, J.; Bai, H.; Zhang, R. Production of Levulinic Acid from Cellulose and Cellulosic Biomass in Different Catalytic Systems. *Catalysts* **2020**, *10*, 1006. [[CrossRef](#)]
22. Rackemann, D.W.; Doherty, W.O.S. The conversion of lignocellulosics to levulinic acid. *Biofuels Bioprod. Biorefin.* **2011**, *5*, 198–214. [[CrossRef](#)]

23. Tian, Y.; Zhang, F.; Wang, J.; Cao, L.; Han, Q. A review on solid acid catalysis for sustainable production of levulinic acid and levulinate esters from biomass derivatives. *Bioresour. Technol.* **2021**, *342*, 125977. [[CrossRef](#)] [[PubMed](#)]
24. Pileidis, F.D.; Titirici, M.-M. Levulinic Acid Biorefineries: New Challenges for Efficient Utilization of Biomass. *ChemSusChem* **2016**, *9*, 562–582. [[CrossRef](#)] [[PubMed](#)]
25. Sajid, M.; Farooq, U.; Bary, G.; Azim, M.M.; Zhao, X. Sustainable production of levulinic acid and its derivatives for fuel additives and chemicals: Progress, challenges, and prospects. *Green Chem.* **2021**, *23*, 9198–9238. [[CrossRef](#)]
26. Signoretto, M.; Taghavi, S.; Ghedini, E.; Menegazzo, F. Catalytic Production of Levulinic Acid (LA) from Actual Biomass. *Molecules* **2019**, *24*, 2760. [[CrossRef](#)] [[PubMed](#)]
27. Gundekari, S.; Srinivasan, K. Chemo- and Regioselective Synthesis of Arylated  $\gamma$ -Valerolactones from Bio-based Levulinic Acid with Aromatics Using H- $\beta$  Zeolite Catalyst. *ChemCatChem* **2019**, *11*, 1102–1111. [[CrossRef](#)]
28. Gundekari, S.; Srinivasan, K. In situ generated Ni(0)@boehmite from NiAl-LDH: An efficient catalyst for selective hydrogenation of biomass derived levulinic acid to gamma-valerolactone. *Catal. Commun.* **2017**, *102*, 40–43. [[CrossRef](#)]
29. Xue, Z.; Liu, Q.; Wang, J.; Mu, T. Valorization of levulinic acid over non-noble metal catalysts: Challenges and opportunities. *Green Chem.* **2018**, *20*, 4391–4408. [[CrossRef](#)]
30. Rodiansono; Astuti, M.D.; Mustikasari, K.; Husain, S.; Ansyah, F.R.; Hara, T.; Shimazu, S. Unravelling the one-pot conversion of biomass-derived furfural and levulinic acid to 1,4-pentanediol catalysed by supported RANEY<sup>®</sup> Ni-Sn alloy catalysts. *RSC Adv.* **2022**, *12*, 241–250. [[CrossRef](#)]
31. Al-Shaal, M.G.; Dzierbinski, A.; Palkovits, R. Solvent-free  $\gamma$ -valerolactone hydrogenation to 2-methyltetrahydrofuran catalysed by Ru/C: A reaction network analysis. *Green Chem.* **2014**, *16*, 1358–1364. [[CrossRef](#)]
32. Gundekari, S.; Srinivasan, K. Hydrous ruthenium oxide: A new generation remarkable catalyst precursor for energy efficient and sustainable production of  $\gamma$ -valerolactone from levulinic acid in aqueous medium. *Appl. Catal. A Gen.* **2019**, *569*, 117–125. [[CrossRef](#)]
33. Martínez Figueredo, K.G.; Virgilio, E.M.; Segobia, D.J.; Bertero, N.M. Valeric Biofuel Production from  $\gamma$ -Valerolactone over Bifunctional Catalysts with Moderate Noble-Metal Loading. *ChemPlusChem* **2021**, *86*, 1342–1346. [[CrossRef](#)] [[PubMed](#)]
34. Zhao, Y.; Fu, Y.; Guo, Q.-X. Production of aromatic hydrocarbons through catalytic pyrolysis of  $\gamma$ -valerolactone from biomass. *Bioresour. Technol.* **2012**, *114*, 740–744. [[CrossRef](#)]
35. Bond, J.Q.; Alonso, D.M.; Wang, D.; West, R.M.; Dumesic, J.A. Integrated Catalytic Conversion of  $\gamma$ -Valerolactone to Liquid Alkenes for Transportation Fuels. *Science* **2010**, *327*, 1110–1114. [[CrossRef](#)] [[PubMed](#)]
36. Gundekari, S.; Srinivasan, K. Screening of Solvents, Hydrogen Source, and Investigation of Reaction Mechanism for the Hydrocyclisation of Levulinic Acid to gamma-Valerolactone Using Ni/SiO<sub>2</sub>-Al<sub>2</sub>O<sub>3</sub> Catalyst. *Catal. Lett.* **2019**, *149*, 215–227. [[CrossRef](#)]
37. Vobecka, Z.; Wei, C.; Tauer, K.; Esposito, D. Poly( $\alpha$ -methylene- $\gamma$ -valerolactone) 1. Sustainable monomer synthesis and radical polymerization studies. *Polymer* **2015**, *74*, 262–271. [[CrossRef](#)]
38. Liu, Q.; Zhao, Z.; Arai, M.; Zhang, C.; Liu, K.; Shi, R.; Wu, P.; Wang, Z.; Lin, W.; Cheng, H.; et al. Transformation of  $\gamma$ -valerolactone into 1,4-pentanediol and 2-methyltetrahydrofuran over Zn-promoted Cu/Al<sub>2</sub>O<sub>3</sub> catalysts. *Catal. Sci. Technol.* **2020**, *10*, 4412–4423. [[CrossRef](#)]
39. Lang, M.; Li, H. Sustainable Routes for the Synthesis of Renewable Adipic Acid from Biomass Derivatives. *ChemSusChem* **2022**, *15*, e202101531. [[CrossRef](#)]
40. Strappaveccia, G.; Ismalaj, E.; Petrucci, C.; Lanari, D.; Marrocchi, A.; Drees, M.; Facchetti, A.; Vaccaro, L. A biomass-derived safe medium to replace toxic dipolar solvents and access cleaner Heck coupling reactions. *Green Chem.* **2015**, *17*, 365–372. [[CrossRef](#)]
41. Petricci, E.; Risi, C.; Ferlin, F.; Lanari, D.; Vaccaro, L. Avoiding hot-spots in Microwave-assisted Pd/C catalysed reactions by using the biomass derived solvent gamma-Valerolactone. *Sci. Rep.* **2018**, *8*, 10571. [[CrossRef](#)]
42. Benisvy-Aharonovich, E.; Zandany, A.; Saady, A.; Kinel-Tahan, Y.; Yehoshua, Y.; Gedanken, A. An efficient method to produce 1,4-pentanediol from the biomass of the algae *Chlorella ohadi* with levulinic acid as intermediate. *Bioresour. Technol. Rep.* **2020**, *11*, 100514. [[CrossRef](#)] [[PubMed](#)]
43. Pace, V.; Hoyos, P.; Castoldi, L.; Domínguez de María, P.; Alcántara, A.R. 2-Methyltetrahydrofuran (2-MeTHF): A Biomass-Derived Solvent with Broad Application in Organic Chemistry. *ChemSusChem* **2012**, *5*, 1369–1379. [[CrossRef](#)] [[PubMed](#)]
44. Tripathi, R.; Lee, C.; Fernandes, R.X.; Olivier, H.; Curran, H.J.; Mani Sarathy, S.; Pitsch, H. Ignition characteristics of 2-methyltetrahydrofuran: An experimental and kinetic study. *Proc. Combust. Inst.* **2017**, *36*, 587–595. [[CrossRef](#)]
45. Alorku, K.; Shen, C.; Li, Y.; Xu, Y.; Wang, C.; Liu, Q. Biomass-derived 2-methyltetrahydrofuran platform: A focus on precious and non-precious metal-based catalysts for the biorefinery. *Green Chem.* **2022**, *24*, 4201–4236. [[CrossRef](#)]
46. Peske, E.A.; Foerster, I.M.; Seames, W.S. Scale-Up for the Conversion of Corn Stover-Derived Levulinic Acid into 2-Methyltetrahydrofuran. *Catalysts* **2023**, *13*, 972. [[CrossRef](#)]
47. Victor, A.; Sharma, P.; Pulidindi, I.N.; Gedanken, A. Levulinic Acid Is a Key Strategic Chemical from Biomass. *Catalysts* **2022**, *12*, 909. [[CrossRef](#)]
48. Liu, P.; Sun, L.; Jia, X.; Zhang, C.; Zhang, W.; Song, Y.; Wang, H.; Li, C. Efficient one-pot conversion of furfural into 2-methyltetrahydrofuran using non-precious metal catalysts. *Mol. Catal.* **2020**, *490*, 110951. [[CrossRef](#)]
49. Date, N.S.; Hengne, A.M.; Huang, K.-W.; Chikate, R.C.; Rode, C.V. One Pot Hydrogenation of Furfural to 2-Methyl Tetrahydrofuran over Supported Mono- and Bi-metallic Catalysts. *ChemistrySelect* **2020**, *5*, 9590–9600. [[CrossRef](#)]

50. Obregón, I.; Gandarias, I.; Al-Shaal, M.G.; Mevissen, C.; Arias, P.L.; Palkovits, R. The Role of the Hydrogen Source on the Selective Production of  $\gamma$ -Valerolactone and 2-Methyltetrahydrofuran from Levulinic Acid. *ChemSusChem* **2016**, *9*, 2488–2495. [[CrossRef](#)]
51. Gan, L.; Deng, J. Catalytic hydrodeoxygenation of neat levulinic acid into 2-methyltetrahydrofuran using a cobalt phosphine complex and Sc(OTf)<sub>3</sub> co-catalytic system. *Green Chem.* **2023**, *25*, 4536–4543. [[CrossRef](#)]
52. Obregón, I.; Gandarias, I.; Miletic, N.; Ocio, A.; Arias, P.L. One-Pot 2-Methyltetrahydrofuran Production from Levulinic Acid in Green Solvents Using Ni-Cu/Al<sub>2</sub>O<sub>3</sub> Catalysts. *ChemSusChem* **2015**, *8*, 3483–3488. [[CrossRef](#)] [[PubMed](#)]
53. Upare, P.P.; Lee, J.-M.; Hwang, Y.K.; Hwang, D.W.; Lee, J.-H.; Halligudi, S.B.; Hwang, J.-S.; Chang, J.-S. Direct Hydrocyclization of Biomass-Derived Levulinic Acid to 2-Methyltetrahydrofuran over Nanocomposite Copper/Silica Catalysts. *ChemSusChem* **2011**, *4*, 1749–1752. [[CrossRef](#)] [[PubMed](#)]
54. Sicaire, A.G.; Vian, M.; Fine, F.; Joffre, F.; Carre, P.; Tostain, S.; Chemat, F. Alternative bio-based solvents for extraction of fat and oils: Solubility prediction, global yield, extraction kinetics, chemical composition and cost of manufacturing. *Int. J. Mol. Sci.* **2015**, *16*, 8430–8453. [[CrossRef](#)] [[PubMed](#)]
55. Aycock, D.F. Solvent Applications of 2-Methyltetrahydrofuran in Organometallic and Biphasic Reactions. *Org. Process Res. Dev.* **2007**, *11*, 156–159. [[CrossRef](#)]
56. Sicaire, A.-G.; Vian, M.A.; Filly, A.; Li, Y.; Bily, A.; Chemat, F. 2-Methyltetrahydrofuran: Main Properties, Production Processes, and Application in Extraction of Natural Products. In *Alternative Solvents for Natural Products Extraction*; Chemat, F., Vian, M.A., Eds.; Springer: Berlin/Heidelberg, Germany, 2014; pp. 253–268.
57. Monticelli, S.; Castoldi, L.; Murgia, I.; Senatore, R.; Mazzeo, E.; Wackerlig, J.; Urban, E.; Langer, T.; Pace, V. Recent advancements on the use of 2-methyltetrahydrofuran in organometallic chemistry. *Monatsh. Chem.* **2017**, *148*, 37–48. [[CrossRef](#)] [[PubMed](#)]
58. Fenard, Y.; Boumehdi, M.A.; Vanhove, G. Experimental and kinetic modeling study of 2-methyltetrahydrofuran oxidation under engine-relevant conditions. *Combust. Flame* **2017**, *178*, 168–181. [[CrossRef](#)]
59. Li, S.; Huang, C.; Yang, C.; Yu, W.; Liu, J.; Zhang, T. A Reduced Reaction Mechanism for Diesel/2-Methyltetrahydrofuran Dual-Fuel Engine Application. *Energies* **2022**, *15*, 7677. [[CrossRef](#)]
60. Jad, Y.E.; Acosta, G.A.; Govender, T.; Kruger, H.G.; El-Faham, A.; de la Torre, B.G.; Albericio, F. Green Solid-Phase Peptide Synthesis 2. 2-Methyltetrahydrofuran and Ethyl Acetate for Solid-Phase Peptide Synthesis under Green Conditions. *ACS Sustain. Chem. Eng.* **2016**, *4*, 6809–6814. [[CrossRef](#)]
61. Khoo, H.H.; Wong, L.L.; Tan, J.; Isoni, V.; Sharratt, P. Synthesis of 2-methyl tetrahydrofuran from various lignocellulosic feedstocks: Sustainability assessment via LCA. *Resour. Conserv. Recycl.* **2015**, *95*, 174–182. [[CrossRef](#)]
62. Kar, Y.; Deveci, H. Importance of P-Series Fuels for Flexible-Fuel Vehicles (FFVs) and Alternative Fuels. *Energy Sources Part A Recovery Util. Environ. Eff.* **2006**, *28*, 909–921. [[CrossRef](#)]
63. Wan Osman, W.N.A.; Badrol, N.A.I.; Samsuri, S. Biodiesel Purification by Solvent-Aided Crystallization Using 2-Methyltetrahydrofuran. *Molecules* **2023**, *28*, 1512. [[CrossRef](#)] [[PubMed](#)]
64. Xiao, H.; Zeng, P.; Li, Z.; Zhao, L.; Fu, X. Combustion performance and emissions of 2-methylfuran diesel blends in a diesel engine. *Fuel* **2016**, *175*, 157–163. [[CrossRef](#)]
65. Obregón, I.; Gandarias, I.; Arias, P.L. 2-Methyl Tetrahydrofuran (MTHF) and its Use as Biofuel. In *Furfural (Chapter 3.5)*; World Scientific: Chennai, India, 2018; pp. 137–155.
66. Zhang, N.; Sun, C.; Huang, Y.; Zhu, C.; Wu, Z.; Lv, L.; Zhou, X.; Wang, X.; Xiao, X.; Fan, X.; et al. Tuning electrolyte enables microsized Sn as an advanced anode for Li-ion batteries. *J. Mater. Chem. A* **2021**, *9*, 1812–1821. [[CrossRef](#)]
67. Koch, V.R.; Young, J.H. 2-Methyltetrahydrofuran—Lithium Hexafluoroarsenate: A Superior Electrolyte for the Secondary Lithium Electrode. *Science* **1979**, *204*, 499–501. [[CrossRef](#)] [[PubMed](#)]
68. Arakawa, M.; Tobishima, S.; Hirai, T.; Yamaki, J. Effect of purification of 2-methyltetrahydrofuran/ethylene carbonate mixed solvent electrolytes on cyclability of lithium metal anodes for rechargeable cells. *J. Appl. Electrochem.* **1999**, *29*, 1191–1196. [[CrossRef](#)]
69. Lei, P.; Ling, Y.; An, J.; Nolan, S.P.; Szostak, M. 2-Methyltetrahydrofuran (2-MeTHF): A Green Solvent for Pd–NHC-Catalyzed Amide and Ester Suzuki-Miyaura Cross-Coupling by N–C/O–C Cleavage. *Adv. Synth. Catal.* **2019**, *361*, 5654–5660. [[CrossRef](#)]
70. Rajkiewicz, A.A.; Skowerski, K.; Trzaskowski, B.; Kajetanowicz, A.; Grela, K. 2-Methyltetrahydrofuran as a Solvent of Choice for Spontaneous Metathesis/Isomerization Sequence. *ACS Omega* **2019**, *4*, 1831–1837. [[CrossRef](#)] [[PubMed](#)]
71. Alcantara, A.R.; de Maria, P.D. Recent Advances on the Use of 2-methyltetrahydrofuran (2-MeTHF) in Biotransformations. *Curr. Green Chem.* **2018**, *5*, 86–103. [[CrossRef](#)]
72. Jad, Y.E.; Acosta, G.A.; Khattab, S.N.; de la Torre, B.G.; Govender, T.; Kruger, H.G.; El-Faham, A.; Albericio, F. 2-Methyltetrahydrofuran and cyclopentyl methyl ether for green solid-phase peptide synthesis. *Amino Acids* **2016**, *48*, 419–426. [[CrossRef](#)]
73. Parris, P.; Duncan, J.N.; Fleetwood, A.; Beierschmitt, W.P. Calculation of a permitted daily exposure value for the solvent 2-methyltetrahydrofuran. *Regul. Toxicol. Pharmacol.* **2017**, *87*, 54–63. [[CrossRef](#)]
74. Antonucci, V.; Coleman, J.; Ferry, J.B.; Johnson, N.; Mathe, M.; Scott, J.P.; Xu, J. Toxicological Assessment of 2-Methyltetrahydrofuran and Cyclopentyl Methyl Ether in Support of Their Use in Pharmaceutical Chemical Process Development. *Org. Process Res. Dev.* **2011**, *15*, 939–941. [[CrossRef](#)]
75. Cue, B.W.; Zhang, J. Green process chemistry in the pharmaceutical industry. *Green Chem. Lett. Rev.* **2009**, *2*, 193–211. [[CrossRef](#)]

76. Pace, V.; Hoyos, P.; Fernández, M.; Sinisterra, J.V.; Alcántara, A.R. 2-Methyltetrahydrofuran as a suitable green solvent for phthalimide functionalization promoted by supported KF. *Green Chem.* **2010**, *12*, 1380–1382. [[CrossRef](#)]
77. Musarurwa, H.; Tavengwa, N.T. Supramolecular solvent-based micro-extraction of pesticides in food and environmental samples. *Talanta* **2021**, *223*, 121515. [[CrossRef](#)] [[PubMed](#)]
78. Cañadas, R.; González-Miquel, M.; González, E.J.; Díaz, I.; Rodríguez, M. Evaluation of bio-based solvents for phenolic acids extraction from aqueous matrices. *J. Mol. Liq.* **2021**, *338*, 116930. [[CrossRef](#)]
79. Tobishima, S.-I.; Hayashi, K.; Nemoto, Y.; Yamaki, J.-I. Ethylene carbonate/propylene carbonate/2-methyl-tetrahydrofuran ternary mixed solvent electrolyte for rechargeable lithium/amorphous V2O5-P2O5 cells. *Electrochim. Acta* **1997**, *42*, 1709–1716. [[CrossRef](#)]
80. Sasaki, Y.; Hosoya, M.; Handa, M. Lithium cycling efficiency of ternary solvent electrolytes with ethylene carbonate—Dimethyl carbonate mixture. *J. Power Sources* **1997**, *68*, 492–496. [[CrossRef](#)]
81. Hu, J.Z.; Jaegers, N.R.; Hahn, N.T.; Hu, W.; Han, K.S.; Chen, Y.; Sears, J.A.; Murugesan, V.; Zavadil, K.R.; Mueller, K.T. Understanding the Solvation-Dependent Properties of Cyclic Ether Multivalent Electrolytes Using High-Field NMR and Quantum Chemistry. *JACS Au* **2022**, *2*, 917–932. [[CrossRef](#)] [[PubMed](#)]
82. Geysens, P.; Lin, P.-C.; Franssaer, J.; Binnemans, K. Electrodeposition of neodymium and dysprosium from organic electrolytes. *Phys. Chem. Chem. Phys.* **2021**, *23*, 9070–9079. [[CrossRef](#)]
83. Pan, F.; Wang, Q. Redox Species of Redox Flow Batteries: A Review. *Molecules* **2015**, *20*, 20499–20517. [[CrossRef](#)]
84. Huang, R.; Yu, C.; Patureau, F.W. Electrochemical Dehydrogenative Acetalization Protection of Alcohols with Tetrahydrofuran. *ChemElectroChem* **2021**, *8*, 3943–3946. [[CrossRef](#)]
85. Englezou, G.; Kortsens, K.; Pacheco, A.A.C.; Cavanagh, R.; Lentz, J.C.; Krumins, E.; Sanders-Velez, C.; Howdle, S.M.; Nedoma, A.J.; Taresco, V. 2-Methyltetrahydrofuran (2-MeTHF) as a versatile green solvent for the synthesis of amphiphilic copolymers via ROP, FRP, and RAFT tandem polymerizations. *J. Polym. Sci.* **2020**, *58*, 1571–1581. [[CrossRef](#)]
86. Bednarek, M.; Kubisa, P. Cationic polymerization of 2-hydroxymethyltetrahydrofuran. *J. Polym. Sci. Part A Polym. Chem.* **2006**, *44*, 6484–6493. [[CrossRef](#)]
87. Stadler, B.M.; Tin, S.; Kux, A.; Grauke, R.; Koy, C.; Tiemersma-Wegman, T.D.; Hinze, S.; Beck, H.; Glocker, M.O.; Brandt, A.; et al. Co-Oligomers of Renewable and “Inert” 2-MeTHF and Propylene Oxide for Use in Bio-Based Adhesives. *ACS Sustain. Chem. Eng.* **2020**, *8*, 13467–13480. [[CrossRef](#)]
88. Narasimhan, V.; Lloyd, D.R.; Burns, C.M. Phase equilibria of polystyrene/polybutadiene/tetrahydrofuran using gel permeation chromatography. *J. Appl. Polym. Sci.* **1979**, *23*, 749–754. [[CrossRef](#)]
89. Yoshikawa, T.; Kimura, K.; Fujimura, S. The gel permeation chromatography of phenolic compounds. *J. Appl. Polym. Sci.* **1971**, *15*, 2513–2520. [[CrossRef](#)]
90. Mrkvičková, L.; Lopour, P.; Pokorný, S.; Janča, J. Gel permeation chromatography of polyisobutylene in tetrahydrofuran. *Die Angew. Makromol. Chem.* **1980**, *90*, 217–221. [[CrossRef](#)]
91. Samorì, C.; Pitacco, W.; Vagnoni, M.; Catelli, E.; Collorichio, T.; Gualandi, C.; Mantovani, L.; Mezzi, A.; Sciutto, G.; Galletti, P. Recycling of multilayer packaging waste with sustainable solvents. *Resour. Conserv. Recycl.* **2023**, *190*, 106832. [[CrossRef](#)]
92. Anderson, L.; Yu, E.; Chen, W.-T. Chemical Recycling of Mixed Plastics in Electronic Waste Using Solvent-Based Processing. *Processes* **2021**, *10*, 66. [[CrossRef](#)]
93. Bernardoni, F.; Halsey, H.M.; Hartman, R.; Nowak, T.; Regalado, E.L. Generic gas chromatography flame ionization detection method using hydrogen as the carrier gas for the analysis of solvents in pharmaceuticals. *J. Pharm. Biomed. Anal.* **2019**, *165*, 366–373. [[CrossRef](#)]
94. de Jesus, S.S.; Ferreira, G.F.; Moreira, L.S.; Wolf Maciel, M.R.; Maciel Filho, R. Comparison of several methods for effective lipid extraction from wet microalgae using green solvents. *Renew. Energy* **2019**, *143*, 130–141. [[CrossRef](#)]
95. Laitinen, A.T.; Parsana, V.M.; Jauhiainen, O.; Huotari, M.; van den Broeke, L.J.P.; de Jong, W.; Vlught, T.J.H.; Ramdin, M. Liquid–Liquid Extraction of Formic Acid with 2-Methyltetrahydrofuran: Experiments, Process Modeling, and Economics. *Ind. Eng. Chem. Res.* **2021**, *60*, 5588–5599. [[CrossRef](#)]
96. Bermudez, J.M.; Menendez, J.A.; Romero, A.A.; Serrano, E.; Garcia-Martinez, J.; Luque, R. Continuous flow nanocatalysis: Reaction pathways in the conversion of levulinic acid to valuable chemicals. *Green Chem.* **2013**, *15*, 2786–2792. [[CrossRef](#)]
97. Phanopoulos, A.; White, A.J.P.; Long, N.J.; Miller, P.W. Catalytic Transformation of Levulinic Acid to 2-Methyltetrahydrofuran Using Ruthenium–N-Triphos Complexes. *ACS Catal.* **2015**, *5*, 2500–2512. [[CrossRef](#)]
98. Patankar, S.C.; Yadav, G.D. Cascade engineered synthesis of  $\gamma$ -valerolactone, 1,4-pentanediol and 2-methyltetrahydrofuran from levulinic acid using novel Pd-Cu/ZrO<sub>2</sub> catalyst and water as solvent. *ACS Sustain. Chem. Eng.* **2015**, *3*, 2619–2630. [[CrossRef](#)]
99. Mizugaki, T.; Togo, K.; Maeno, Z.; Mitsudome, T.; Jitsukawa, K.; Kaneda, K. One-Pot Transformation of Levulinic Acid to 2-Methyltetrahydrofuran Catalyzed by Pt–Mo/H- $\beta$  in Water. *ACS Sustain. Chem. Eng.* **2016**, *4*, 682–685. [[CrossRef](#)]
100. Upare, P.P.; Lee, M.; Lee, S.-K.; Yoon, J.W.; Bae, J.; Hwang, D.W.; Lee, U.H.; Chang, J.-S.; Hwang, Y.K. Ru nanoparticles supported graphene oxide catalyst for hydrogenation of bio-based levulinic acid to cyclic ethers. *Catal. Today* **2016**, *265*, 174–183. [[CrossRef](#)]
101. Zheng, J.; Zhu, J.; Xu, X.; Wang, W.; Li, J.; Zhao, Y.; Tang, K.; Song, Q.; Qi, X.; Kong, D.; et al. Continuous hydrogenation of ethyl levulinate to  $\gamma$ -valerolactone and 2-methyl tetrahydrofuran over alumina doped Cu/SiO<sub>2</sub> catalyst: The potential of commercialization. *Sci. Rep.* **2016**, *6*, 28898. [[CrossRef](#)] [[PubMed](#)]

102. Licursi, D.; Antonetti, C.; Fulignati, S.; Giannoni, M.; Raspolli Galletti, A.M. Cascade Strategy for the Tunable Catalytic Valorization of Levulinic Acid and  $\gamma$ -Valerolactone to 2-Methyltetrahydrofuran and Alcohols. *Catalysts* **2018**, *8*, 277. [[CrossRef](#)]
103. Novodárszki, G.; Solt, H.E.; Valyon, J.; Lónyi, F.; Hancsók, J.; Deka, D.; Tuba, R.; Mihályi, M.R. Selective hydroconversion of levulinic acid to  $\gamma$ -valerolactone or 2-methyltetrahydrofuran over silica-supported cobalt catalysts. *Catal. Sci. Technol.* **2019**, *9*, 2291–2304. [[CrossRef](#)]
104. Xie, Z.; Chen, B.; Wu, H.; Liu, M.; Liu, H.; Zhang, J.; Yang, G.; Han, B. Highly efficient hydrogenation of levulinic acid into 2-methyltetrahydrofuran over Ni–Cu/Al<sub>2</sub>O<sub>3</sub>–ZrO<sub>2</sub> bifunctional catalysts. *Green Chem.* **2019**, *21*, 606–613. [[CrossRef](#)]
105. Gu, C.; Chen, L.; Liu, Y.; Zhang, X.; Liu, J.; Zhang, Q.; Wang, C.; Ma, L. One-pot conversion of biomass-derived levulinic acid to furanic biofuel 2-methyltetrahydrofuran over bimetallic NiCo/ $\gamma$ -Al<sub>2</sub>O<sub>3</sub> catalysts. *Mol. Catal.* **2022**, *524*, 112317. [[CrossRef](#)]

**Disclaimer/Publisher’s Note:** The statements, opinions and data contained in all publications are solely those of the individual author(s) and contributor(s) and not of MDPI and/or the editor(s). MDPI and/or the editor(s) disclaim responsibility for any injury to people or property resulting from any ideas, methods, instructions or products referred to in the content.